Memory-Event-Triggered H_∞ Load Frequency Control of Multi-Area Power Systems With Cyber-Attacks and Communication Delays

Shen Yan, Zhou Gu, and Ju H. Park, *Senior Member, IEEE*

***Abstract*—This article focuses on H_∞ load frequency control (LFC) of multi-area power systems with cyber-attacks and communication delays by a memory-event-triggered mechanism (METM). The dynamics of power system components, such as governor, turbine and power generator, are imitated by some circuit systems. To save the precious network bandwidth, a METM is constructed to decide which measured data should be transmitted as the control signal. In contrast to some memoryless ETMs, the proposed METM uses historic data over a fixed period. To guarantee no Zeno behavior, a positive constant time is waited after each trigger happens. By treating the exchanges of tie-line power between the ith control area and other areas as exogenous disturbances, a novel decentralized distributed delay system is modeled to represent the decentralized H_∞ LFC of a multi-area power system under the proposed METM with deception attacks and communication delays. By selecting a Lyapunov-Krasovskii functional (LKF) based on the distributed delay terms, new sufficient criterions are obtained to co-design the H_∞ LFC controller and triggering parameters for power systems against deception attacks. Finally, the advantages of the presented method is shown via an illustrative case.**

***Index Terms*—Cyber-attacks, load frequency control, memory event-triggered mechanism, power systems.**

I. Introduction

In POWER systems, load frequency control (LFC) is an effective manner to ensure the electric power quality by regulating the frequency at desired values [1]–[4]. In a multi-area power system, power exchanges among different areas by tie-lines make the frequency regulation difficult. In contrast to the centralized LFC strategy using the global system information, a decentralized control scheme only utilizing the information of local area is more practical and feasible. For LFC strategy, when the area frequency deviates from the equilibrium point, the deviation will be used as the control signal to adapt the valve opening of the governor, which changes the steam flow into the steam turbine. Then the rotor speed of the power generator is regulated to drive the generated power frequency to a steady value. Recently, the networked control strategy has been applied successfully in power systems, where the communication among system components such as plants, sensors, controllers and actuators is over the network channels. The networked LFC issues of power systems have been studied and some effective controller design methods have been provided in some published results [5], [6]. In practical environment, the limited network channel bandwidth could induce network congestion when tremendous data communications happen, which may degrade the control performance even cause system instability.

To overcome the above problem, event-triggered mechanism (ETM) has been recognized as a preferable strategy to save precious network resources. This strategy is executed by designing a suitable triggering condition to choose "necessary" data as the control signal [7]–[11]. As a result, a great deal of outcomes about LFC power systems with ETM can be found in [12]–[15] and the references therein. To name a few, [12] addresses the event-triggered LFC problem of power systems with transmission delays by using a time delay system method. In [13], the static output frequency control issue for time-delay power systems is investigated, in which electric vehicles are considered in control strategy to suppress fluctuations of frequency induced by load changes. Compared with some ETMs with constant triggering threshold parameter, an adaptive event-triggered LFC issue of power systems is developed in [14] by designing a dynamic triggering threshold. Different from the above ETMs based on sampled data (also called discrete-time ETM), a switching ETM [16] between a waiting period and a continuous-time ETM is utilized in frequency regulation for power systems with time-varying communication delays in [15]. However, the PI controller gains K_P and K_I in [15] are given in advance, which can not be co-designed with the system performance. In addition, it is worthy noting that most of these ETMs use the instantaneous measured output and last triggered data to construct the triggering rules.

Manuscript received January 10, 2021; revised February 18, 2021; accepted March 6, 2021. Date of publication March 9, 2021; date of current version July 7, 2021. This work was supported in part by the Natural Science Foundation of Jiangsu Province of China under Grant BK20200769, in part by the Natural Science Foundation of Jiangsu Provincial Universities under Grant 20KJB510045, and in part by the National Natural Science Foundation of China under Grants 61473156 and 52005266. The work of Ju H. Park was supported by the National Research Foundation of Korea (NRF) grant funded by the Korea government (MSIT) under Grant 2020R1A2B5B02002002. Recommended for acceptance by Prof. Shouhuai Xu. *(Corresponding authors: Zhou Gu and Ju H. Park.)*

Shen Yan and Zhou Gu are with the College of Mechanical and Electronic Engineering, Nanjing Forestry University, Nanjing 210037, China (e-mail: yanshenzdh@gmail.com; gzh1808@163.com).

Ju H. Park is with the Department of Electrical Engineering, Yeungnam University, Kyongsan 38541, South Korea (e-mail: jessie@ynu.ac.kr).

Digital Object Identifier 10.1109/TNSE.2021.3064933

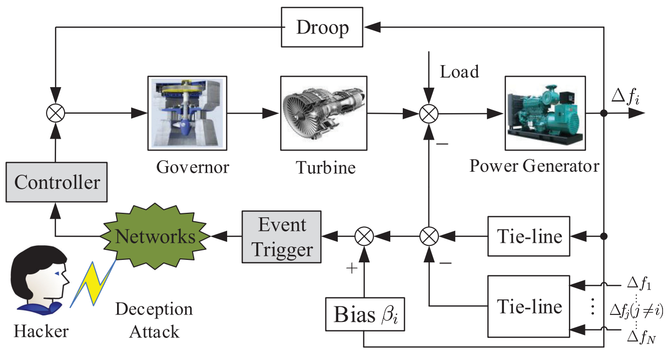

Fig. 1. The structure of the ith control area of a multi-area event-triggered LFC system .

Practically, the measured output could have stochastic fluctuations incurred by exogenous noises and disturbances [17], [18]. Under such situation, the existing ETMs are sensitive to the fluctuations, which may trigger many unnecessary data to over-occupy limited network bandwidth. [17] proposes the idea of adding the historic information into the triggering condition, which is verified to be valid for decreasing the triggered times by some numerical examples. [19] extends the above ETM into an unmanned surface vehicle system subject to failures, and designs a fault detection filter. This work also shows that the ETM based on historic information is helpful for saving the network bandwidth. Nevertheless, communication delays are not taken into consideration in [17]. Moreover, the integral term induced by the mean of outputs in [17] is handled via an approximation method, which could lead to approximation error. Therefore, the first motivation of this work is how to remove the approximation error for the event-triggered LFC power systems with communication delays.

On the other line, due to the utilization of open networks to communicate signals, power systems are exposed to the threaten and risk of attacks from network, like Denial-of-service (DoS) attacks [21], [22] and deception attacks [23], [24]. For instance, a nuclear power station of Iranian is damaged by StuxNet virus, which affects about 60% hosts. Consequently, the security issue of power systems has gained much researchers' attention and fruitful results have been reported in [25]–[27]. Generally speaking, considering the case of DoS attacks with finite energy, a resilient event-triggered LFC method for power systems is developed in [25]. A resilient LFC approach is addressed in [26] for power systems subject to deception attacks with a new ETM, which is sensitive to the external disturbances. [27] proposes a hybrid attack model, including both DoS attacks and deception attacks, and studies the issue of LFC for power systems under an event-based communication mechanism. Nevertheless, less effort has been devoted to the event-triggered H_∞ LFC issue of power systems with deception attacks by using the past outputs, which is another motivation of this study.

Motivated by above observations, this paper is concerned with the decentralized event-triggered H_∞ LFC of a multi-area power system against deception attacks and communication delays. The contributions are summarized as:

1) The system components such as governor, turbine and power generator are imitated by some circuits, of which the dynamics can be described via some differential equations based on circuit analysis. Then the ith subsystem is transformed to a circuit system composed by several resistors, capacitors and operational amplifiers (OAs). Meanwhile, the controller is also imitated by two circuit systems. By choosing appropriate states, the state-space system model of the ith area subsystem can be established from these differential equations.

2) The historic system outputs in a given time interval are utilized to design a novel METM. Compared with some existing ETMs only using current system information, the presented METM can avoid more redundant triggered data induced by random changes of measured outputs.

3) The event-triggered LFC system with communication delays is modeled as a switched system between a time-varying distributed delay system and a time-varying delay system, where a waiting time period is introduced into the METM to avoid Zeno behavior. Then, by adopting a new LKF related with the time-varying distributed delay terms and a less conservative integral inequality technique, the existence of a decentralized event-triggered H_∞ load frequency controller is ensured by some sufficient linear matrix inequality conditions.

The organization of this paper is given as follows. Section II provides the system modeling and problem statement. The main results on the event-triggered H_∞ LFC of multi-area power systems under cyber-attacks are obtained in Section III. Simulation results are executed in Section IV. Conclusions are summarized in Section V.

Notation: In this article, Y^T means the transpose of a matrix or vector Y. $*$ stands for $[*]XY = Y^TXY$ or $\begin{bmatrix} X & Y \\ Y^T & Z \end{bmatrix} = \begin{bmatrix} X & Y \\ * & Z \end{bmatrix}$. He$(Y)$ equals to $Y^T + Y$. $\otimes$ means Kronecker product.

II. Preliminaries

For a multi-area power system with N control areas, we consider a simplified subsystem i comprising of governor, non-reheated turbine, and power generator (see Fig. 1, where $\Delta f_i(t)$ is the frequency deviation) [12], [15]. In this paper, a circuit system model composed by resistors, capacitors and operational amplifiers (OAs) (see Fig. 2) is utilized to imitate the dynamics of generator, turbine and governor. Signals and parameters of the ith circuit system model are shown in Table I.

For the ith control area, based on Kirchhoff Voltage Law and Kirchhoff Current Law, the dynamics of the governor imitated by a circuit with resistor R_{gi}, capacitor C_{gi} and operational amplifier OA1 can be described as:

$$\begin{cases} R_{gi} i_{gi} = \frac{R_{f1i} u_{fi}(t)}{R_{f2i}} - u_i(t) \\ i_{gi} = i_{gi1} + i_{gi2} \\ i_{gi1} = -\frac{u_{gi}(t)}{R_{gi}} \\ i_{gi2} = -C_{gi} \dot{u}_{gi}(t) \end{cases}, \tag{1}$$

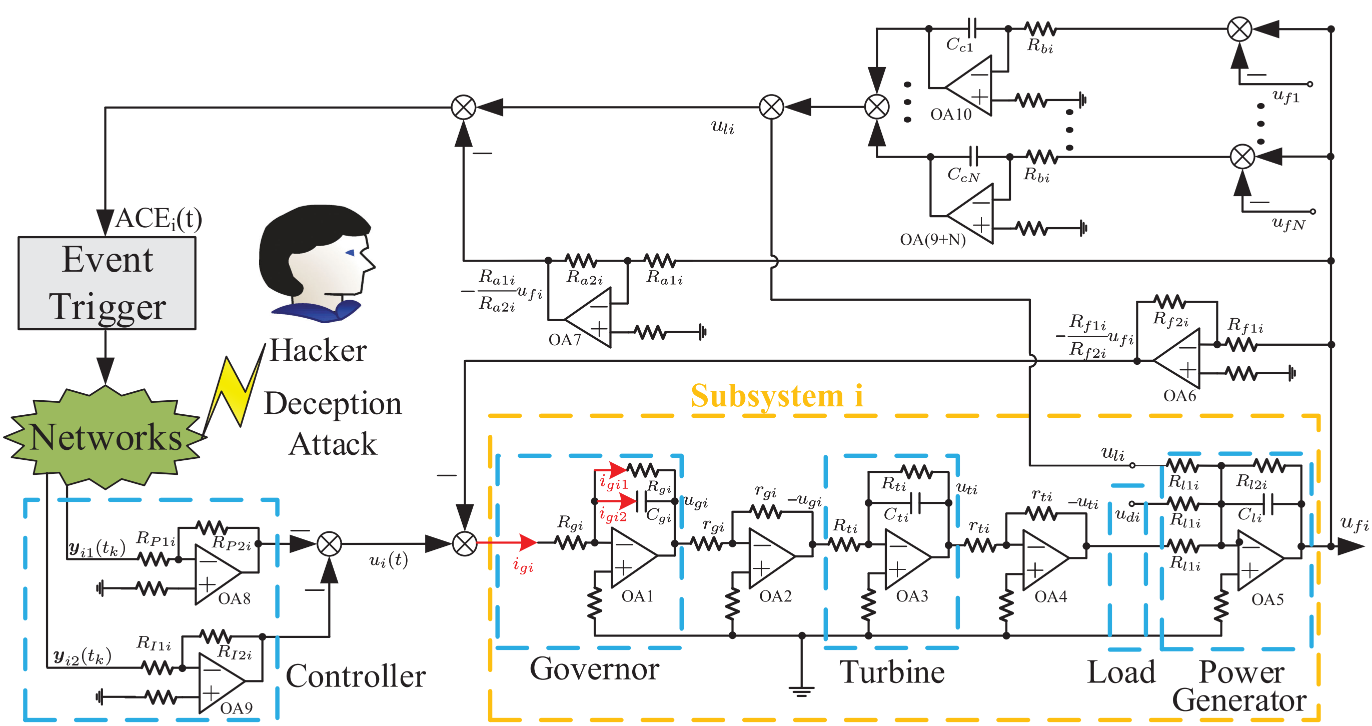

Fig. 2. The dynamic model of the ith control area of a multi-area event-triggered LFC system imitated by circuit systems.

which is written as the following differential equation:

$$\dot{u}_{gi}(t) = -\frac{u_{gi}(t)}{R_{gi}C_{gi}} - \frac{R_{f1i}}{R_{f2i}}\frac{u_{fi}(t)}{R_{gi}C_{gi}} + \frac{1}{R_{gi}C_{gi}}u_i(t) \tag{2}$$

Applying the same analysis procedure to turbine and generator, the dynamic model of system plant can be derived as:

$$\begin{cases} \dot{u}_{fi}(t) = -\frac{R_{l1i}}{R_{l2i}}\frac{u_{fi}(t)}{R_{li1}C_{li}} + \frac{u_{ti}(t)-u_{di}(t)-u_{li}(t)}{R_{li1}C_{li}} \\ \dot{u}_{ti}(t) = -\frac{u_{ti}(t)}{R_{ti}C_{ti}} + \frac{u_{gi}(t)}{R_{ti}C_{ti}} \\ \dot{u}_{gi}(t) = -\frac{u_{gi}(t)}{R_{gi}C_{gi}} - \frac{R_{f1i}}{R_{f2i}}\frac{u_{fi}(t)}{R_{gi}C_{gi}} + \frac{1}{R_{gi}C_{gi}}u_i(t) \\ \dot{u}_{li}(t) = \sum_{j=1,j\neq i}^{N}\frac{1}{R_{bi}C_{cj}}(u_{fi}(t) - u_{fj}(t)) \end{cases}, \tag{3}$$

The area control error (ACE) of the ith area is defined as:

$$ACE_i(t) = \beta_i u_{fi}(t) + u_{li}(t), \tag{4}$$

where β_i is the frequency bias factor.

By choosing state vector, output vector, disturbance (load) as $\boldsymbol{x}_i(t) = [u_{fi}(t), u_{ti}(t), u_{gi}(t), \int_0^t ACE_i(s)ds, u_{li}(t)]^T \in \mathbb{R}^5$, $\boldsymbol{y}_i(t) = [ACE_i(t), \int_0^t ACE_i(s)ds]^T \in \mathbb{R}^2$ and $\varpi_i(t) = [u_{di}(t), \eta_i(t)]^T \in \mathbb{R}^2$ $(\eta_i(t) = \sum_{j=1,j\neq i}^{N}\mathcal{T}_{ij}u_{fj}(t))$, respectively, the state-space model of the ith LFC system is established as:

$$\begin{cases} \dot{\boldsymbol{x}}_i(t) = \boldsymbol{A}_i\boldsymbol{x}_i(t) + \boldsymbol{B}_i\boldsymbol{u}_i(t) + \boldsymbol{F}_i\boldsymbol{\varpi}_i(t) \\ \boldsymbol{y}_i(t) = \boldsymbol{C}_i\boldsymbol{x}_i(t) \\ \boldsymbol{z}_i(t) = \boldsymbol{H}_i\boldsymbol{x}_i(t) \end{cases}, \tag{5}$$

where the measured output $\boldsymbol{y}_i(t)$ is also the performance output $z_i(t)$. $\boldsymbol{A}_i$, $\boldsymbol{B}_i$, $\boldsymbol{C}_i$, $\boldsymbol{F}_i$ and $\boldsymbol{H}_i$ are known system matrices and given as

$$\boldsymbol{A}_i = \begin{bmatrix} -\frac{\mathcal{D}_i}{\mathcal{M}_i} & \frac{1}{\mathcal{M}_i} & 0 & 0 & -\frac{1}{\mathcal{M}_i} \\ 0 & -\frac{1}{\mathcal{T}_{ti}} & \frac{1}{\mathcal{T}_{ti}} & 0 & 0 \\ \frac{-1}{\mathcal{R}_{fi}\mathcal{T}_{gi}} & 0 & -\frac{1}{\mathcal{T}_{gi}} & 0 & 0 \\ \beta_i & 0 & 0 & 0 & 1 \\ \sum_{j=1,j\neq i}^{N}\mathcal{T}_{ij} & 0 & 0 & 0 & 0 \end{bmatrix}, \boldsymbol{B}_i = \begin{bmatrix} 0 \\ 0 \\ \frac{1}{\mathcal{T}_{gi}} \\ 0 \\ 0 \end{bmatrix},$$

$$\boldsymbol{F}_i^T = \begin{bmatrix} -\frac{1}{\mathcal{M}_i} & 0 & 0 & 0 & 0 \\ 0 & 0 & 0 & 0 & -1 \end{bmatrix}^T, \ \boldsymbol{C}_i = \begin{bmatrix} \beta_i & 0 & 0 & 0 & 0 \\ 0 & 0 & 0 & 1 & 0 \end{bmatrix},$$

$$\boldsymbol{H}_i = \boldsymbol{C}_i, \ \beta_i = \frac{R_{a1i}}{R_{a2i}}, \ \mathcal{T}_{ij} = \frac{1}{R_{bi}C_{cj}}, \ \mathcal{D}_i = \frac{R_{l1i}}{R_{l2i}},$$

$$\mathcal{M}_i = R_{li1}C_{li}, \ \mathcal{T}_{ti} = R_{ti}C_{ti}, \ \mathcal{T}_{gi} = R_{gi}C_{gi}, \ \mathcal{R}_{fi} = \frac{R_{f1i}}{R_{f2i}},$$

where $\mathcal{T}_{gi}$ and $\mathcal{T}_{ti}$ represent the time constants of the governor and turbine, respectively; $\mathcal{D}_i$ and $\mathcal{M}_i$, mean the damping coefficient and inertia moment of generator, respectively; $\mathcal{R}_{fi}$ is the droop coefficient; $\mathcal{T}_{ij}$ means the tie line synchronizing coefficient for area i and j.

Utilizing ACE as the input of a PI controller, one has:

$$\boldsymbol{u}_i(t) = K_{Pi}ACE_i(t) + K_{Ii}\int_0^t ACE_i(s)ds = \boldsymbol{K}_i\boldsymbol{y}_i(t), \tag{6}$$

where $\boldsymbol{K}_i = [K_{Pi} \ \ K_{Ii}]$ is the controller gain, K_{Pi} and K_{Ii} are the proportional and integral gains, respectively.

To mitigate the burden of communication network, the following METM is presented to decide the next transmitting time of control signal:

TABLE I
SIGNALS AND PARAMETERS IN FIG. 2 OF THE CIRCUIT SYSTEM MODEL OF THE iTH CONTROL AREA

Symbol	Nomenclatures
OA	Operational amplifier
R_{gi}, C_{gi}	Resistor and capacitor in OA1
i_{gi}, i_{g1i}, i_{g2i}	Branch currents in OA1
u_{gi}	Terminal voltage in OA1
R_{ti}, C_{ti}	Resistor and capacitor in OA3
u_{ti}	Terminal voltage in OA3
r_{gi}, r_{ti}	Resistors in OA2 and OA4
R_{l1i}, R_{l2i}, C_{li}	Resistors and capacitor in OA5
u_{fi}	Terminal voltage in OA5
R_{f1i}, R_{f2i}	Resistors in OA6
R_{a1i}, R_{a2i}	Resistors in OA7
R_{P1i}, R_{P2i}	Resistors in OA8
R_{I1i}, R_{I2i}	Resistors in OA9
R_{bi}, C_{cj}	Resistor and capacitor in OA(9+j), $j=1,\cdots,N$, $j\neq i$
u_{li}	Sum of the terminal voltages in OA(9+j)
u_{di}	Equivalent voltage source of load

$$t_{k+1} = \sup_t\big\{t \geq t_k + \tau|[*]\Psi_i \boldsymbol{e}_i(t) \leq \sigma_i[*]\Psi_i \boldsymbol{y}_i^*(t)\big\}, \quad (7)$$

where $\boldsymbol{y}_i^*(t) \triangleq \frac{1}{h}\int_{t-h}^{t} \boldsymbol{y}_i(s)ds$, $\boldsymbol{e}_i(t) = \boldsymbol{y}^*(t) - \boldsymbol{y}_i(t_k)$, t_k and t_{k+1} are the latest and next triggering times, respectively, $\sigma_i \in [0,\ 1)$ is the triggering threshold parameter, $\Psi_i > 0$ is a weighting matrix, $\tau > 0$ is a waiting time period and $h > 0$ stands for an interval of past outputs.

Remark 1: In practical applications, the measured output may include some stochastic fluctuations induced by disturbances or noises. Under this situation, some existing ETMs [15], [16] based on instantaneous system output $\boldsymbol{y}_i(t)$ could be affected by such fluctuations and generate tremendous data packets. To decrease the effect of random fluctuations, the integral signal $\boldsymbol{y}_i^*(t)$ over a given time interval h is utilized to design the triggering condition. As a result, more precious network resources could be economized via the presented METM than the conventional ETMs [15], [16]. Moreover, the integral signal $\boldsymbol{y}_i^*(t)$ can be derived by an analog RC integral circuit system composed by operational amplifier, resistors, capacitors and time delay module.

Remark 2: When the time interval is chosen as $h \to 0$, (7) reduces to

$$t_{k+1} = \sup_t\{t \geq t_k + \tau|[*]\Psi_i \tilde{\boldsymbol{e}}_i(t) \leq \sigma_i[*]\Psi_i \boldsymbol{y}_i(t)\} \quad (8)$$

with $\tilde{\boldsymbol{e}}_i(t) = \boldsymbol{y}_i(t) - \boldsymbol{y}_i(t_k)$, which is equivalent to the switching ETM [15], [16] and [28] with $C_i = I$. That is to say, the presented METM is more general than some ETMs studied in existing results.

Remark 3: In order to avoid Zeno phenomenon (infinite triggered events in finite time), it needs to prove that there exists a positive minimum inter-event interval. In some existing event-triggered control systems [29], [30], a criterion is developed to compute the lower bound on inter-event interval. Without the complex computation of inter-event interval, a positive time interval τ is waited after each event triggered by the proposed METM, which can be viewed as the lower bound on inter-event interval. Then, Zeno phenomenon is excluded naturally.

By considering the network communication delays, the input of controller $\hat{\boldsymbol{y}}_i(t)$ ($t \in [t_k + \theta_k,\ t_{k+1} + \theta_{k+1})$) is expressed as

$$\hat{\boldsymbol{y}}_i(t) = \boldsymbol{y}_i(t_k), \quad (9)$$

where θ_k is the communication delay with upper bound $\bar{\theta}$.

Then, (9) can be further presented as

$$\hat{\boldsymbol{y}}_i(t) = \begin{cases} \boldsymbol{y}_i(t-\tau(t)), & t \in [t_k + \theta_k,\ t_k + \theta_k + \tau) \\ \tilde{\boldsymbol{y}}_i(t), & t \in [t_k + \theta_k + \tau,\ t_{k+1} + \theta_{k+1}) \end{cases}, \quad (10)$$

where

$$\begin{aligned} &\tau(t) = t - t_k \leq h + \tau \triangleq \bar{\tau}, \\ &\tilde{\boldsymbol{y}}_i(t) = \frac{1}{h}\int_{t-\theta(t)-h}^{t-\theta(t)} \boldsymbol{y}_i(s)ds - \boldsymbol{\epsilon}_i(t), \\ &\boldsymbol{\epsilon}_i(t) = \boldsymbol{e}_i(t-\theta(t)), \\ &\theta(t) = \frac{t_{k+1} + \theta_{k+1} - t}{t_{k+1} + \theta_{k+1} - t_k - \theta_k - \tau}\theta_k \\ &\qquad + \frac{t - t_k}{t_{k+1} + \theta_{k+1} - t_k - \theta_k - \tau}\theta_{k+1} \leq \bar{\theta}. \end{aligned}$$

Remark 4: The time-varying term $\theta(t)$ defined in (10) is a "fictitious" delay. To use the event-triggering condition, the similar way in [16] is taken to choose such $\theta(t)$ in (10) that the proposed METM (7) implies

$$[*]\Psi_i \boldsymbol{\epsilon}_i(t) \leq \sigma_i[*]\Psi_i \boldsymbol{y}_i^*(t-\theta(t))$$

with $\boldsymbol{y}_i^*(t-\theta(t)) = \frac{1}{h}\int_{t-\theta(t)-h}^{t-\theta(t)} \boldsymbol{y}_i(s)ds$ for $t \in [t_k + \theta_k + \tau,\ t_{k+1} + \theta_{k+1})$. With this treatment, the proposed METM and the considered time-varying delays can be handled in the united framework of time-varying distributed delay system.

By defining a novel time-varying variable $\eta(t) \triangleq \theta(t) + h$, $\eta(t) \leq \bar{\eta} \triangleq \bar{\theta} + h$, $\tilde{\boldsymbol{y}}_i(t)$ is further written as

$$\tilde{\boldsymbol{y}}_i(t) = \frac{1}{h}\left(\int_{t-\eta(t)}^{t} \boldsymbol{y}_i(s)ds - \int_{t-\theta(t)}^{t} \boldsymbol{y}_i(s)ds\right) - \boldsymbol{\epsilon}_i(t).$$

Meanwhile, the signal transmitted over the communication network is vulnerable to be attacked by adversaries. By considering the deception attack, the controller is further expressed as:

$$\boldsymbol{u}_i^a(t) = \boldsymbol{K}_i(\hat{\boldsymbol{y}}_i(t) + \boldsymbol{d}_i(t)), \quad (11)$$

where $\boldsymbol{d}_i(t)$ is the deception attack to change the control signal and satisfies

$$\|\boldsymbol{d}_i(t)\|_2 \leq \|\boldsymbol{D}_i \boldsymbol{y}_i(t)\|_2 \quad (12)$$

with a constant known matrix $\boldsymbol{D}_i$.

By substituting (11) and (15) into system (5), the resulting LFC system with the proposed METM is derived as:

$$\begin{aligned}\dot{\boldsymbol{x}}_i(t) = &\boldsymbol{A}_i\boldsymbol{x}_i(t) + (1-\chi(t))\boldsymbol{B}_i\boldsymbol{K}_i\boldsymbol{C}_i\boldsymbol{x}_i(t-\tau(t))\\ &+ \chi(t)\frac{\boldsymbol{B}_i\boldsymbol{K}_i\boldsymbol{C}_i}{h}\left(\int_{t-\eta(t)}^{t}\boldsymbol{x}_i(s)ds - \int_{t-\theta(t)}^{t}\boldsymbol{x}_i(s)ds\right)\\ &- \chi(t)\boldsymbol{B}_i\boldsymbol{K}_i\epsilon_i(t) + \boldsymbol{B}_i\boldsymbol{K}_i\boldsymbol{d}_i(t) + \boldsymbol{F}_i\boldsymbol{\varpi}_i(t),\end{aligned} \tag{13}$$

where

$$\chi(t) = \begin{cases}0, & t\in[t_k+\theta_k,\ t_k+\theta_k+\tau)\\ 1, & t\in[t_k+\theta_k+\tau,\ t_{k+1}+\theta_{k+1})\end{cases}.$$

The purpose of this paper is to design the decentralized controller (11) such that

1) When $\varpi_i(t)=0$, the exponential stability of the ith LFC system (13) is ensured;

2) When $\varpi_i(t)\neq 0$ and $\boldsymbol{x}_i(0)=0$, the H_∞ performance $\int_0^\infty z_i^T(t)z_i(t)dt < \gamma_i^2\int_0^\infty \varpi_i^T(t)\varpi_i(t)dt$ is ensured with a prescribed $\gamma_i > 0$.

For further proceeding, the following definition and lemma are presented to obtain the main results.

Definition 1: [35] The Legendre polynomials defined over the interval $[a,\ b]$ are given as

$$L_m(s)\triangleq(-1)^m\sum_{n=0}^{m}P_n^m\left(\frac{s-a}{b-a}\right)^n$$

with $P_n^m=(-1)^n\binom{m}{n}\binom{m+n}{j}$.

Some properties are presented as:

1) Orthogonality: $\forall\kappa\in\mathbb{N},\ \int_a^b\mathcal{L}_\kappa^T(s)\mathcal{L}_\kappa(s)ds=\frac{1}{b-a}W_\kappa$, where $\mathcal{L}_\kappa(s)\triangleq[\,L_0(s)\ \cdots\ L_m(s)\ \cdots\ L_\kappa(s)\,]^T$ and $W_\kappa=diag\{1,3,\ldots,2\kappa+1\}$;

2) Bound: $\forall i\in\mathbb{N},\ L_m(b)=1,\ \ L_m(a)=(-1)^m$;

3) Differentiation: for $m=0$, $\dot{L}_m(s)=0$; and for $m\geq 1$, $\dot{L}_m(s)=\sum_{k=0}^{m-1}\frac{(2m+1)}{b-a}(1-(-1)^{m+k})$.

Lemma 1: [31] For a given function $x(v)\in\mathbb{R}^q$, $v\in[a,\ b]$, a matrix $R\in\mathbb{R}^{q\times q} > 0$, the following inequality

$$\int_a^b[*]Rx(s)ds\geq\frac{1}{b-a}[*](\mathcal{R}\otimes W_\kappa)\left(\begin{bmatrix}\mathbb{K}_{q,(\kappa+1)} & 0_{(\kappa+1)q}\\ 0_{(\kappa+1)q} & \mathbb{K}_{q,(\kappa+1)}\end{bmatrix}L_\kappa\right) \tag{14}$$

holds for any $S\in\mathbb{R}^{q\times q}$ satisfying $\mathcal{R}>0,\ \ c\in[a,\ b]$, $\mathbb{L}_\kappa(s)\triangleq\mathcal{L}_\kappa(s)\otimes I_q$ with $\mathcal{R}=\begin{bmatrix}R & S\\ * & R\end{bmatrix}$, $L_\kappa=\begin{bmatrix}\int_c^b\mathbb{L}_\kappa(s)x(s)ds\\ \int_a^c\mathbb{L}_\kappa(s)x(s)ds\end{bmatrix}$.

Proof: By choosing $\varpi(s)=1$ and $\mathbf{f}(s)=\mathcal{L}_\kappa(s)$ in Lemma 3 in [31], the above lemma can be obtained directly. ■

Remark 5: The matrix $\mathbb{K}_{q,(\kappa+1)}\in\mathbb{R}^{q(\kappa+1)\times q(\kappa+1)}$ denotes the communication matrix for Kronecker products, which has the same property shown in Lemma 2 in [31]. In addition, $\mathbb{K}_{q,(\kappa+1)}$ can be solved by the Matlab function $\mathbf{vecperm}(q,(\kappa+1))$ given by [32].

III. Main Results

For simplifying the derivations of the main results, we define

$$\mathbb{E}_a^1\triangleq\begin{cases}[\,0_{5,5(a-1)}\ I_5\ 0_{5,5(10+4\kappa-a)+4}\,], & a=1,\ldots,10+4\kappa\\ [\,0_{2,5(10+4\kappa)}\ \ I_2\ \ 0_2\,], & a=11+4\kappa\\ [\,0_{2,5(10+4\kappa)}\ \ 0_2\ \ I_2\,], & a=12+4\kappa\end{cases}$$

$$\mathbb{E}_b^2\triangleq\begin{cases}[\,0_{5,5(b-1)}\ 0_{5,2(b-2)}\ I_5\ 0_{5,5(10+4\kappa-b)+4}\,], & \\ & b=1,2,4,\ldots,10+4\kappa\\ [\,0_{2,10}\ I_2\ 0_{2,5(7+4\kappa)+4}\,], & b=3\\ [\,0_{2,5(9+4\kappa)+2}\ \ I_2\ \ 0_2\,], & b=11+4\kappa\\ [\,0_{2,5(9+4\kappa)+2}\ \ 0_2\ \ I_2\,], & b=12+4\kappa\end{cases}$$

$$L_\kappa^1(t)=\begin{bmatrix}\mathscr{L}_{\kappa,1}^1(t)\\ \mathscr{L}_{\kappa,2}^1(t)\end{bmatrix},\quad L_\kappa^2(t)=\begin{bmatrix}\mathscr{L}_{\kappa,1}^2(t)\\ \mathscr{L}_{\kappa,2}^2(t)\end{bmatrix},$$

$$\mathscr{L}_\kappa^1(t)=\int_{-\bar{\theta}}^{0}\mathbb{L}_\kappa^1(s)\boldsymbol{x}_i(t+s)ds,$$

$$\mathscr{L}_{\kappa,1}^1(t)=\int_{-\theta(t)}^{0}\mathbb{L}_\kappa^1(s)\boldsymbol{x}_i(t+s)ds,$$

$$\mathscr{L}_{\kappa,2}^1(t)=\int_{-\bar{\theta}}^{-\theta(t)}\mathbb{L}_\kappa^1(s)\boldsymbol{x}_i(t+s)ds,$$

$$\mathscr{L}_\kappa^2(t)=\int_{-\bar{\eta}}^{0}\mathbb{L}_\kappa^2(s)\boldsymbol{x}_i(t+s)ds,$$

$$\mathscr{L}_{\kappa,1}^2(t)=\int_{-\eta(t)}^{0}\mathbb{L}_\kappa^2(s)\boldsymbol{x}_i(t+s)ds,$$

$$\mathscr{L}_{\kappa,2}^2(t)=\int_{-\bar{\eta}}^{-\eta(t)}\mathbb{L}_\kappa^2(s)\boldsymbol{x}_i(t+s)ds.$$

By defining $\mathcal{I}=[\,I_5\quad 0_{5,5\kappa}\,]$, one obtains

$$\int_{t-\theta(t)-h}^{t-\theta(t)}\boldsymbol{y}_i(s)ds=\boldsymbol{C}_i\mathcal{I}\Big(\mathcal{L}_{\kappa,1}^2(t)-\mathcal{L}_{\kappa,1}^1(t)\Big). \tag{15}$$

First, the stability analysis conditions for system (13) satisfying H_∞ performance are provided in the following theorem.

Theorem 1: For given parameters σ_i, τ, h, θ, μ_1, μ_2, under the METM (7), the exponential stability with a decay rate λ and an H_∞ performance γ_i of the ith subsystem (13) is guaranteed, if there exist symmetric matrices P_i, $Q_{1i}>0$, $Q_{2i}>0$, $U_{1i}>0$, $U_{2i}>0$, $R_{1i}>0$, $R_{2i}>0$, $\Psi_i>0$, $\mathcal{Q}_{2i}=\begin{bmatrix}Q_{2i} & S_i\\ S_i^T & Q_{2i}\end{bmatrix}>0$, $\mathfrak{R}_{1i}=\begin{bmatrix}R_{1i} & S_{1i}\\ S_{1i}^T & R_{1i}\end{bmatrix}>0$, $\mathfrak{R}_{2i}=\begin{bmatrix}R_{2i} & S_{2i}\\ S_{2i}^T & R_{2i}\end{bmatrix}>0$, $0<Z_i<\nu I$ and matrices $\boldsymbol{K}_i$ and $\boldsymbol{Y}_i$ such that

$$\mathcal{P}_i > 0, \tag{16}$$

$$\Pi_i^1+\Theta_i^1 < 0, \tag{17}$$

$$\Pi_i^2+\Theta_i^2 < 0, \tag{18}$$

where

$$e^{-2\lambda\bar{\tau}} \triangleq e_\tau, \quad e^{-2\lambda\bar{\theta}} \triangleq e_\theta, \quad e^{-2\lambda\bar{\eta}} \triangleq e_\eta,$$

$$\mathcal{P}_i = P_i + diag\{0_5, \frac{e_\theta}{\bar{\theta}}\mathscr{U}_{1i}, \frac{e_\eta}{\bar{\eta}}\mathscr{U}_{2i}, \},$$

$$\mathscr{U}_{1i} = W_\kappa \otimes U_{1i}, \quad \mathscr{U}_{2i} = W_\kappa \otimes U_{2i},$$

$$\mathbf{\Pi}_i^1 = \mathbf{\Gamma}_i^1 + He(\mathscr{Y}_i^1 \mathscr{G}_i^1), \quad \mathscr{Y}_i^1 = (\mu_1 \boldsymbol{Y}_i \mathbb{E}_1^1 + \mu_2 \boldsymbol{Y}_i \mathbb{E}_2^1)^T,$$

$$\mathscr{G}_i^1 = \boldsymbol{A}_i \mathbb{E}_2^1 + \boldsymbol{B}_i \boldsymbol{K}_i \boldsymbol{C}_i \mathbb{E}_3^1 + \boldsymbol{F}_i \mathbb{E}_{11+4\kappa}^1 + \boldsymbol{B}_i \boldsymbol{K}_i \mathbb{E}_{12+4\kappa}^1 - \mathbb{E}_1^1,$$

$$\mathbf{\Gamma}_i^1 = He(\boldsymbol{M}_1^T P_i \boldsymbol{N}_1) + 2\lambda \boldsymbol{M}_1^T P_i \boldsymbol{M}_1 - \frac{e_\tau}{\bar{\tau}} \mathbb{I}_1^T \mathcal{Q}_{2i} \mathbb{I}_1 + \Lambda_i^1,$$

$$\mathbf{\Theta}_i^1 = \mathbb{E}_2^{1\,T}(\nu(\boldsymbol{D}_i \boldsymbol{C}_i)^T \boldsymbol{D}_i \boldsymbol{C}_i + \boldsymbol{C}_i^T \boldsymbol{C}_i)\mathbb{E}_2^1,$$

$$\boldsymbol{M}_1 = \begin{bmatrix} \mathbb{E}_2^1 \\ \mathbb{I}_{\kappa,1}^1 + \mathbb{I}_{\kappa,2}^1 \\ \mathbb{I}_{\kappa,3}^1 + \mathbb{I}_{\kappa,4}^1 \end{bmatrix}, \quad \boldsymbol{N}_1 = \begin{bmatrix} \mathbb{E}_1^1 \\ \mathbf{1}\mathbb{E}_2^1 - \hat{\mathbf{1}}\mathbb{E}_5^1 - \frac{\Lambda_\kappa}{\bar{\theta}}(\mathbb{I}_{\kappa,1}^1 + \mathbb{I}_{\kappa,2}^1) \\ \mathbf{1}\mathbb{E}_2^1 - \hat{\mathbf{1}}\mathbb{E}_6^1 - \frac{\Lambda_\kappa}{\bar{\eta}}(\mathbb{I}_{\kappa,3}^1 + \mathbb{I}_{\kappa,4}^1) \end{bmatrix},$$

$$\mathbb{I}_{\kappa,j}^{1\,T} = \begin{bmatrix} \mathbb{E}_{6+(j+1)\kappa-\kappa}^{1\,T} & \cdots & \mathbb{E}_{6+(j+1)\kappa}^{1\,T} \end{bmatrix}^T, \; j = 1,2,3,4,$$

$$\mathbf{1}^T = [\, I_5 \;\cdots\; I_5 \,]_{5(\kappa+1),5}^T, \quad \hat{\mathbf{1}}^T = [\, (-1)^0 I_5 \;\cdots\; (-1)^\kappa I_5 \,]^T,$$

$$\Lambda_\kappa = \begin{bmatrix} \lambda_0^0 I & \cdots & \lambda_0^\kappa I \\ \vdots & \lambda_g^l & \vdots \\ \lambda_\kappa^0 I & \cdots & \lambda_\kappa^\kappa I \end{bmatrix}, \lambda_g^l = \begin{cases} -(2l+1)(1-(-1)^{g+l}), & l \le g, \\ 0, & l > g, \end{cases}$$

$$\Lambda_i^1 = diag\{\Lambda_{1i}^1, \Lambda_{2i}^1, 0_5, \Lambda_{4i}^1, \Lambda_{5i}^1, \Lambda_{6i}^1, \Lambda_{7i}^1, \Lambda_{8i}^1, \Lambda_{9i}^1, \Lambda_{10i}^1\},$$

$$\Lambda_{1i}^1 = \bar{\tau} Q_{2i}, \quad \Lambda_{2i}^1 = Q_{1i} + U_{1i} + \bar{\theta} R_{1i} + U_{2i} + \bar{\eta} R_{2i},$$

$$\Lambda_{4i}^1 = -e_\tau Q_{1i}, \quad \Lambda_{5i}^1 = -e_\theta U_{1i}, \quad \Lambda_{6i}^1 = -e_\eta U_{2i},$$

$$\Lambda_{7i}^1 = -\frac{e_\theta}{\bar{\theta}} \mathbb{K}^T \mathscr{R}_{1i} \mathbb{K}, \quad \mathscr{R}_{1i} = \mathfrak{R}_{1i} \otimes W_\kappa,$$

$$\Lambda_{8i}^1 = -\frac{e_\eta}{\bar{\eta}} \mathbb{K}^T \mathscr{R}_{2i} \mathbb{K}, \quad \mathscr{R}_{2i} = \mathfrak{R}_{2i} \otimes W_\kappa,$$

$$\mathbf{\Pi}_i^2 = \mathbf{\Gamma}_i^2 + \mathbb{I}_4^T \Phi_i \mathbb{I}_4 + He(\mathscr{Y}_i^2 \mathscr{G}_i^2), \quad \Lambda_{9i}^1 = -\gamma_i^2 I,$$

$$\mathscr{Y}_i^2 = (\mu_1 \boldsymbol{Y}_i \mathbb{E}_1^2 + \mu_2 \boldsymbol{Y}_i \mathbb{E}_2^2)^T, \quad \Lambda_{10i}^1 = -Z_i,$$

$$\mathscr{G}_i^2 = \boldsymbol{A}_i \mathbb{E}_2^2 - \boldsymbol{B}_i \boldsymbol{K}_i \mathbb{E}_3^2 + \frac{1}{h} \boldsymbol{B}_i \boldsymbol{K}_i \boldsymbol{C}_i \mathbb{I}_3 + \boldsymbol{F}_i \mathbb{E}_{11+4\kappa}^2 + \boldsymbol{B}_i \boldsymbol{K}_i \mathbb{E}_{12+4\kappa}^2 - \mathbb{E}_1^2,$$

$$\mathbf{\Gamma}_i^2 = He(\boldsymbol{M}_2^T P_i \boldsymbol{N}_2) + 2\lambda \boldsymbol{M}_2^T P_i \boldsymbol{M}_2 - \frac{e_\tau}{\bar{\tau}} \mathbb{I}_2^T Q_{2i} \mathbb{I}_2 + \Lambda_i^2,$$

$$\mathbf{\Theta}_i^2 = \mathbb{E}_2^{2\,T}(\nu(\boldsymbol{D}_i \boldsymbol{C}_i)^T \boldsymbol{D}_i \boldsymbol{C}_i + \boldsymbol{C}_i^T \boldsymbol{C}_i)\mathbb{E}_2^2,$$

$$\boldsymbol{M}_2 = \begin{bmatrix} \mathbb{E}_2^2 \\ \mathbb{I}_{\kappa,1}^2 + \mathbb{I}_{\kappa,2}^2 \\ \mathbb{I}_{\kappa,3}^2 + \mathbb{I}_{\kappa,4}^2 \end{bmatrix}, \quad \boldsymbol{N}_2 = \begin{bmatrix} \mathbb{E}_1^2 \\ \mathbf{1}\mathbb{E}_1^2 - \hat{\mathbf{1}}\mathbb{E}_5^2 - \frac{\Lambda_\kappa}{\bar{\theta}}(\mathbb{I}_{\kappa,1}^2 + \mathbb{I}_{\kappa,2}^2) \\ \mathbf{1}\mathbb{E}_1^2 - \hat{\mathbf{1}}\mathbb{E}_6^2 - \frac{\Lambda_\kappa}{\bar{\eta}}(\mathbb{I}_{\kappa,3}^2 + \mathbb{I}_{\kappa,4}^2) \end{bmatrix},$$

$$\mathbb{I}_{\kappa,j}^{2\,T} = \begin{bmatrix} \mathbb{E}_{6+(j+1)\kappa-\kappa}^{2\,T} & \cdots & \mathbb{E}_{6+(j+1)\kappa}^{2\,T} \end{bmatrix}^T, \; j = 1,2,3,4,$$

$$\Lambda_i^2 = diag\{\Lambda_{1i}^1, \Lambda_{2i}^1, 0_2, \Lambda_{4i}^1, \Lambda_{5i}^1, \Lambda_{6i}^1, \Lambda_{7i}^1, \Lambda_{8i}^1, \Lambda_{9i}^1, \Lambda_{10i}^1\},$$

$$\mathbb{I}_1 = \begin{bmatrix} \mathbb{E}_2^1 - \mathbb{E}_3^1 \\ \mathbb{E}_3^1 - \mathbb{E}_4^1 \end{bmatrix}, \; \mathbb{I}_2 = \begin{bmatrix} \mathbb{E}_2^2 - \mathbb{E}_4^2 \end{bmatrix}, \; \mathbb{I}_3 = (\mathbb{E}_{9+2\kappa}^2 - \mathbb{E}_7^2),$$

$$\mathbb{I}_4 = \begin{bmatrix} \mathbb{E}_3^2 \\ \mathbb{I}_3 \end{bmatrix}, \Phi_i = \begin{bmatrix} -\mathbf{\Psi}_i & 0_{2,5} \\ 0_{5,2} & \frac{\sigma_i}{h^2} \boldsymbol{C}_i^T \mathbf{\Psi}_i \boldsymbol{C}_i \end{bmatrix}.$$

Proof. We define $\boldsymbol{\xi}_i^T(t) = \begin{bmatrix} \boldsymbol{x}_i^T(t) & \mathscr{L}_\kappa^{1\,T}(t) & \mathscr{L}_\kappa^{2\,T}(t) \end{bmatrix}^T$ and construct an LKF as

$$V_i(t) = \boldsymbol{\xi}_i^T(t) P_i \boldsymbol{\xi}_i(t) + \int_{t-\bar{\tau}}^{t} e^{2\lambda(s-t)} \boldsymbol{x}_i^T(s) Q_{1i} \boldsymbol{x}_i(s) ds + \int_{t-\bar{\theta}}^{t} e^{2\lambda(s-t)} \boldsymbol{x}_i^T(s)[U_{1i} + (s-t+\bar{\theta})R_{1i}]\boldsymbol{x}_i(s) ds + \int_{t-\bar{\eta}}^{t} e^{2\lambda(s-t)} \boldsymbol{x}_i^T(s)[U_{2i} + (s-t+\bar{\eta})R_{2i}]\boldsymbol{x}_i(s) ds + \int_{-\bar{\tau}}^{0}\int_{t+v}^{t} e^{2\lambda(s-t)} \dot{\boldsymbol{x}}_i^T(s) Q_2 \dot{\boldsymbol{x}}_i(s) ds dv. \tag{19}$$

By using Lemma 1 to the selected LKF (19), it gives

$$\int_{-\bar{\theta}}^{0} e^{2\lambda s}[*]U_{1i}\boldsymbol{x}_i(t+s)ds \ge \frac{e_\theta}{\bar{\theta}}[*](W_\kappa \otimes U_{1i})\mathscr{L}_\kappa^1(t), \tag{20}$$

$$\int_{-\bar{\eta}}^{0} e^{2\lambda s}[*]U_{2i}\boldsymbol{x}_i(t+s)ds \ge \frac{e_\eta}{\bar{\eta}}[*](W_\kappa \otimes U_{2i})\mathscr{L}_\kappa^2(t). \tag{21}$$

In terms of (19) and (20), one can get

$$V_i(t) \ge \boldsymbol{\xi}_i^T(t)\mathcal{P}_i\boldsymbol{\xi}_i(t) + \int_{-\bar{\tau}}^{0} e^{2\lambda s}[*]Q_{1i}\boldsymbol{x}_i(t+s)ds + \int_{-\bar{\theta}}^{0} e^{2\lambda s}[*]R_{1i}\boldsymbol{x}_i(t+s)ds + \int_{-\bar{\eta}}^{0} e^{2\lambda s}[*]R_{2i}\boldsymbol{x}_i(t+s)ds + \int_{-\bar{\tau}}^{0}\int_{t+v}^{t} e^{2\lambda(s-t)}[*]Q_{2i}\dot{\boldsymbol{x}}(s)dsdv. \tag{22}$$

Therefore, $V_i(t) > 0$ is guaranteed by $R_{1i} > 0$, $R_{2i} > 0$, $Q_{1i} > 0, Q_{2i} > 0, \mathcal{P}_i > 0$.

Next, the time derivative of LKF is calculated as:

$$\begin{aligned} &\dot{V}_i(t) + 2\lambda V_i(t) \\ &\le 2\boldsymbol{\xi}_i^T(t)P_i\dot{\boldsymbol{\xi}}_i(t) + 2\lambda\boldsymbol{\xi}_i^T(t)P_i\boldsymbol{\xi}_i(t) + \bar{\tau}[*]Q_{2i}\dot{\boldsymbol{x}}_i(t) + [*] \\ &\quad \times (Q_{1i} + U_{1i} + \bar{\theta}R_{1i} + U_{2i} + \bar{\eta}R_{2i})\boldsymbol{x}_i(t) \\ &\quad - e_\tau[*]Q_{1i}\boldsymbol{x}_i(t-\bar{\tau}) - e_\tau\int_{t-\bar{\tau}}^{t}[*]Q_{2i}\dot{\boldsymbol{x}}_i(s)ds \\ &\quad - e_\theta[*]U_{1i}\boldsymbol{x}_i(t-\bar{\theta}) - e_\theta\int_{-\bar{\theta}}^{0}[*]R_{1i}\boldsymbol{x}_i(t+s)ds \\ &\quad - e_\eta[*]U_{2i}\boldsymbol{x}_i(t-\bar{\eta}) - e_\eta\int_{-\bar{\eta}}^{0}[*]R_{2i}\boldsymbol{x}_i(t+s)ds. \end{aligned} \tag{23}$$

Then, to guarantee the exponential stability of the ith LFC subsystem (13) with a given index γ_i, it needs

$$\dot{V}_i(t)+2\lambda V_i(t)+z_i^T(t)z_i(t)-\gamma_i^2\boldsymbol{\varpi}_i^T(t)\boldsymbol{\varpi}_i(t)\leq\mathcal{J}_i(t)<0, \quad (24)$$

where

$$\begin{aligned}\mathcal{J}_i(t)\triangleq&2\boldsymbol{\xi}_i^T(t)P_i\dot{\boldsymbol{\xi}}_i(t)+2\lambda\boldsymbol{\xi}_i^T(t)P_i\boldsymbol{\xi}_i(t)+\bar{\tau}\dot{\boldsymbol{x}}_i^T(t)Q_{2i}\dot{\boldsymbol{x}}_i(t)\\&+\boldsymbol{x}_i^T(t)(Q_{1i}+U_{1i}+\bar{\theta}R_{1i}+U_{2i}+\bar{\eta}R_{2i}+\boldsymbol{C}_i^T\boldsymbol{C}_i)\boldsymbol{x}_i(t)\\&-\gamma_i^2\boldsymbol{\varpi}_i^T(t)\boldsymbol{\varpi}_i(t)-e_\tau[*]Q_{1i}\boldsymbol{x}_i(t-\bar{\tau})-e_\tau\int_{t-\bar{\tau}}^{t}[*]Q_{2i}\dot{\boldsymbol{x}}_i(s)ds\\&-e_\theta[*]U_{1i}\boldsymbol{x}_i(t-\bar{\theta})-e_\theta\int_{-\bar{\theta}}^{0}[*]R_{1i}\boldsymbol{x}_i(t+s)ds\\&-e_\eta[*]U_{2i}\boldsymbol{x}_i(t-\bar{\eta})-e_\eta\int_{-\bar{\eta}}^{0}[*]R_{2i}\boldsymbol{x}_i(t+s)ds.\end{aligned}$$

With the help of Lemma 1, the last two integral terms in (24) can be relaxed as:

$$-e_\theta\int_{-\bar{\theta}}^{0}[*]R_{1i}\boldsymbol{x}_i(t+s)ds\leq-\frac{e_\theta}{\bar{\theta}}[*]\mathbb{K}^T\mathscr{R}_{1i}\mathbb{K}L_\kappa^1(t), \quad (25)$$

$$-e_\eta\int_{-\bar{\eta}}^{0}[*]R_{2i}\boldsymbol{x}_i(t+s)ds\leq-\frac{e_\eta}{\bar{\eta}}[*]\mathbb{K}^T\mathscr{R}_{2i}\mathbb{K}L_\kappa^2(t). \quad (26)$$

According to (12) and $0<Z_i<\nu I$, one can get

$$\nu\boldsymbol{x}^T(t)(\boldsymbol{D}_i\boldsymbol{C}_i)^T\boldsymbol{D}_i\boldsymbol{C}_i\boldsymbol{x}_i(t)-\boldsymbol{d}_i^T(t)Z_i\boldsymbol{d}_i(t)\geq0 \quad (27)$$

Next, two cases where the system (13) is operated over the time interval $t\in[t_k+\theta_k,\ t_k+\tau+\theta_k)$ and the time interval $t\in[t_k+\tau+\theta_k,t_{k+1}+\theta_{k+1})$ are considered, respectively.

Case I ($\chi(t)=1$): The system (13) is given as:

$$\begin{aligned}\dot{\boldsymbol{x}}_i(t)=&\boldsymbol{A}_i\boldsymbol{x}_i(t)+\boldsymbol{B}_i\boldsymbol{K}_i\boldsymbol{C}_i\boldsymbol{x}_i(t-\tau(t))\\&+\boldsymbol{B}_i\boldsymbol{K}_i\boldsymbol{d}_i(t)+\boldsymbol{F}_i\boldsymbol{\varpi}_i(t).\end{aligned} \quad (28)$$

Define $\boldsymbol{\zeta}_{1i}^T(t)=\Big[\dot{\boldsymbol{x}}_i^T(t)\ \ \boldsymbol{x}_i^T(t)\ \ \boldsymbol{x}_i^T(t-\tau(t))\ \ \boldsymbol{x}_i^T(t-\bar{\tau})\ \ \boldsymbol{x}_i^T(t-\bar{\theta})\ \ \boldsymbol{x}_i^T(t-\bar{\eta})\ \ L_\kappa^{1\,T}(t)\ \ L_\kappa^{2\,T}(t)\ \ \boldsymbol{\varpi}_i^T(t)\ \ \boldsymbol{d}_i^T(t)\Big]$.

Thus, the system (28) can be reformed as:

$$\mathscr{G}_i^1\boldsymbol{\zeta}_{1i}(t)=0. \quad (29)$$

Based on the bound property and differentiation property of $L_i(v)$, we have

$$\dot{\mathscr{L}}_\kappa^1(t)=\mathbf{1}\boldsymbol{x}_i(t)-\hat{\mathbf{1}}\boldsymbol{x}_i(t-\bar{\theta})-\frac{\Lambda_\kappa}{\bar{\theta}}(\mathscr{L}_{\kappa,1}^1(t)+\mathscr{L}_{\kappa,2}^1(t)), \quad (30)$$

$$\dot{\mathscr{L}}_\kappa^2(t)=\mathbf{1}\boldsymbol{x}_i(t)-\hat{\mathbf{1}}\boldsymbol{x}_i(t-\bar{\eta})-\frac{\Lambda_\kappa}{\bar{\eta}}(\mathscr{L}_{\kappa,1}^2(t)+\mathscr{L}_{\kappa,2}^2(t)). \quad (31)$$

$\boldsymbol{\xi}_i(t)$ and $\dot{\boldsymbol{\xi}}_i(t)$ also can be denoted as:

$$\boldsymbol{\xi}_i(t)=\boldsymbol{M}_1\boldsymbol{\zeta}_{1i}(t),\quad\dot{\boldsymbol{\xi}}_i(t)=\boldsymbol{N}_1\boldsymbol{\zeta}_{1i}(t). \quad (32)$$

Based on $\mathcal{Q}_{2i}>0$ and applying the reciprocally convex lemma [33] to handle $-e_\tau\int_{t-\bar{\tau}}^{t}[*]Q_{2i}\dot{\boldsymbol{x}}_i(s)ds$, it yields

$$-e_\tau\int_{t-\bar{\tau}}^{t}[*]Q_{2i}\dot{\boldsymbol{x}}_i(s)ds\leq-\frac{e_\tau}{\bar{\tau}}[*](\mathbb{I}_1^T\mathcal{Q}_{2i}\mathbb{I}_1)\boldsymbol{\zeta}_{1i}(t). \quad (33)$$

From (25), (27), (32) and (33), (24) is ensured by

$$\boldsymbol{\zeta}_{1i}^T(t)(\Gamma_i^1+\Theta_i^1)\boldsymbol{\zeta}_{1i}(t)<0. \quad (34)$$

From (29) and the construction of $\mathscr{Y}_i^1=(\mu_1\boldsymbol{Y}_i\mathbb{E}_1^1+\mu_2\boldsymbol{Y}_i\mathbb{E}_2^1)^T$, one can derive

$$\boldsymbol{\zeta}_{1i}^T(t)He(\mathscr{Y}_i^1\mathscr{G}_i^1)\boldsymbol{\zeta}_{1i}(t)=0. \quad (35)$$

By substituting (45) into (44), it leads to

$$\boldsymbol{\zeta}_{1i}^T(t)(\Pi_i^1+\Theta_i^1)\boldsymbol{\zeta}_{1i}(t)<0, \quad (36)$$

which is equivalent to (17), where $\Pi_i^1=\Gamma_i^1+He(\mathscr{Y}_i^1\mathscr{G}_i^1)$.

From (46) and (17), one obtains

$$\dot{V}_i(t)+2\lambda V_i(t)\leq-\boldsymbol{z}_i^T(t)\boldsymbol{z}_i(t)+\gamma_i^2\boldsymbol{\varpi}_i^T(t)\boldsymbol{\varpi}_i(t). \quad (37)$$

Case II ($\chi(t)=0$): The system (13) is given as:

$$\begin{aligned}\dot{\boldsymbol{x}}_i(t)=&\boldsymbol{A}_i\boldsymbol{x}_i(t)+\frac{1}{h}\boldsymbol{B}_i\boldsymbol{K}_i\boldsymbol{C}_i\mathcal{I}\Big(\mathcal{L}_{\kappa,1}^2(t)-\mathcal{L}_{\kappa,1}^1(t)\Big)\\&-\boldsymbol{B}_i\boldsymbol{K}_i\boldsymbol{\epsilon}_i(t)+\boldsymbol{B}_i\boldsymbol{K}_i\boldsymbol{d}_i(t).\end{aligned} \quad (38)$$

Define $\boldsymbol{\zeta}_{2i}^T(t)=\Big[\dot{\boldsymbol{x}}_i^T(t)\ \ \boldsymbol{x}_i^T(t)\ \ \boldsymbol{\epsilon}_i^T(t)\ \ \boldsymbol{x}_i^T(t-\bar{\tau})\ \ \boldsymbol{x}_i^T(t-\bar{\theta})\ \ \boldsymbol{x}_i^T(t-\bar{\eta})\ \ L_\kappa^{1\,T}(t)\ \ L_\kappa^{2\,T}(t)\ \ \boldsymbol{\varpi}_i^T(t)\ \ \boldsymbol{d}_i^T(t)\Big]$.

With the above definition, system (38) is shown as:

$$\mathscr{G}_i^2\boldsymbol{\zeta}_{2i}(t)=0. \quad (39)$$

$\boldsymbol{\xi}_i(t)$ and $\dot{\boldsymbol{\xi}}_i(t)$ are expressed as

$$\boldsymbol{\xi}_i(t)=\boldsymbol{M}_2\boldsymbol{\zeta}_{2i}(t),\quad\dot{\boldsymbol{\xi}}_i(t)=\boldsymbol{N}_2\boldsymbol{\zeta}_{2i}(t). \quad (40)$$

By using Jensen inequality [34], it results in

$$-e_\tau\int_{t-\bar{\tau}}^{t}[*]Q_{2i}\dot{\boldsymbol{x}}_i(s)ds\leq-\frac{e_\tau}{\bar{\tau}}[*](\mathbb{I}_2^TQ_{2i}\mathbb{I}_2)\boldsymbol{\zeta}_{2i}(t). \quad (41)$$

Based on $\mathcal{L}_{\kappa,1}^2(t)-\mathcal{L}_{\kappa,1}^1(t)=\mathbb{I}_3\boldsymbol{\zeta}_{2i}(t)$, $\boldsymbol{\epsilon}_i(t)=\mathbb{E}_3^2\boldsymbol{\zeta}_{2i}(t)$, (15) and the triggering condition (7), one has

$$\frac{\sigma_i}{h^2}[*]\Psi_i(\boldsymbol{C}_i\mathbb{I}_3\boldsymbol{\zeta}_{2i}(t))-[*]\Psi_i\boldsymbol{\epsilon}_i(t)=[*](\mathbb{I}_4^T\Phi_i\mathbb{I}_4)\boldsymbol{\zeta}_{2i}(t)>0. \quad (42)$$

Utilizing (42) to (24), we need

$$\begin{aligned}&\dot{V}_i(t)+2\lambda V_i(t)+z_i^T(t)z_i(t)-\gamma_i^2\varpi_i^T(t)\varpi_i(t)\\&\quad+[*]\Psi_i\epsilon_i(t)-[*]\Psi_i\epsilon_i(t)\\&\quad\le\mathcal{J}_i(t)+[*](\mathbb{I}_4^T\Phi_i\mathbb{I}_4)\zeta_{2i}(t)<0.\end{aligned}\tag{43}$$

From (25), (27), (40), (41) and (43), (24) is ensured by

$$\zeta_{2i}^T(t)(\Gamma_i^2+\Theta_i^2)\zeta_{2i}(t)<0.\tag{44}$$

In terms of (39) and the construction of $\mathscr{Y}_i^2=(\mu_1 Y_i\mathbb{E}_1^2+\mu_2 Y_i\mathbb{E}_2^2)^T$, one can derive

$$\zeta_{2i}^T(t)He(\mathscr{Y}_i^2\mathscr{G}_i^2)\zeta_{2i}(t)=0.\tag{45}$$

By adding (45) to (44), it yields

$$\zeta_{2i}^T(t)(\Pi_i^2+\Theta_i^2)\zeta_{2i}(t)<0,\tag{46}$$

which is further ensured via (18), where $\Pi_i^2=\Gamma_i^2+He(\mathscr{Y}_i^2\mathscr{G}_i^2)$.

Thus, it is easy to obtain (37) for Case II.

Then integrating both sides of (37) from 0 to ∞ gives

$$V_i(\infty)-V_i(0)\le\int_0^\infty\left(\gamma_i^2\varpi_i^T(t)\varpi_i(t)-z_i^T(t)z_i(t)\right)dt.\tag{47}$$

If $\varpi_i(t)=0$, one has $\dot{V}_i(t)+2\lambda V_i(t)<0$ from (24). Hence the system (13) is exponentially stable with a decay rate λ. Moreover, we have $\int_0^\infty z_i^T(t)z_i(t))dt\le\gamma_i^2\int_0^\infty\varpi_i^T(t)\varpi_i(t)dt$ under $x_i(0)=0$. These fulfill the proof.

Remark 6: According to the condition (16), it does not need the matrix P_i to be positive to guarantee a positive LKF (19). This treatment could reduce the conservativeness of the stability conditions than the existing results in [20] based on all positive Lyapunov matrices.

Remark 7: Compared to the method based on Simpson's rule in [17], [19] to approximate the distributed delay term induced by METM, it is utilized directly by our method based on Legendre polynomials in Lemma 1, which removes the approximation error introduced by Simpson's rule.

Next, in terms of the results in Theorem 1, sufficient conditions are developed in Theorem 2 to design an event-triggered H_∞ load frequency controller.

Theorem 2: For given parameters σ_i, τ, h, θ, μ_1, μ_2, δ and ρ, under the METM (7), the exponential stability with a decay rate λ and an H_∞ performance γ_i of the ith subsystem (13) is ensured, if there exist symmetric matrices $\tilde{P}_i$, $\tilde{Q}_{1i}>0$, $\tilde{Q}_{2i}>0$, $\tilde{U}_{1i}>0$, $\tilde{U}_{2i}>0$, $\tilde{R}_{1i}>0$, $\tilde{R}_{2i}>0$, $\tilde{\Psi}_i>0$, $\tilde{\mathcal{Q}}_{2i}=\begin{bmatrix}\tilde{Q}_{2i}&\tilde{S}_i\\\tilde{S}_i^T&\tilde{Q}_{2i}\end{bmatrix}>0$, $\tilde{\mathfrak{R}}_{1i}=\begin{bmatrix}\tilde{R}_{1i}&\tilde{S}_{1i}\\\tilde{S}_{1i}^T&\tilde{R}_{1i}\end{bmatrix}>0$, $\tilde{\mathfrak{R}}_{2i}=\begin{bmatrix}\tilde{R}_{2i}&\tilde{S}_{2i}\\\tilde{S}_{2i}^T&\tilde{R}_{2i}\end{bmatrix}>0$, $\mathcal{Z}_i>\nu^{-1}I$ and X_i, L_i and G_i such that

$$\tilde{\mathcal{P}}_i>0,\tag{48}$$

$$\begin{bmatrix}\tilde{\Pi}_i^1&\mathbb{E}_2^{1\,T}X_iC_i^T&\mathbb{E}_2^{1\,T}X_i(\nu D_iC_i)^T\\ *&-I&0\\ *&*&-\nu I\end{bmatrix}<0,\tag{49}$$

$$\begin{bmatrix}\tilde{\Pi}_i^2&\mathbb{E}_2^{2\,T}X_iC_i^T&\mathbb{E}_2^{2\,T}X_i(\nu D_iC_i)^T\\ *&-I&0\\ *&*&-\nu I\end{bmatrix}<0,\tag{50}$$

$$\begin{bmatrix}-\delta I&(G_iC_i-C_iX_i)^T\\G_iC_i-C_iX_i&-I\end{bmatrix}<0,\tag{51}$$

where

$$\begin{aligned}&\tilde{\mathcal{P}}_i=\tilde{P}_i+diag\{0_5,\frac{e_\theta}{\bar{\theta}}\tilde{\mathscr{U}}_{1i},\frac{e_\eta}{\bar{\eta}}\tilde{\mathscr{U}}_{2i},\},\\&\tilde{\mathscr{U}}_{1i}=W_\kappa\otimes\tilde{U}_{1i},\quad\tilde{\mathscr{U}}_{2i}=W_\kappa\otimes\tilde{U}_{2i},\\&\tilde{\Pi}_i^1=\tilde{\Gamma}_i^1+He(\tilde{\mathscr{Y}}_i^1\tilde{\mathscr{G}}_i^1),\quad\tilde{\mathscr{Y}}_i^1=(\mu_1\mathbb{E}_1^1+\mu_2\mathbb{E}_2^1)^T,\\&\tilde{\mathscr{G}}_i^1=A_iX_i\mathbb{E}_2^1+B_iL_i\left(C_i\mathbb{E}_3^1+\mathbb{E}_{12+4\kappa}^1\right)+F_i\mathbb{E}_{11+4\kappa}^1-X_i\mathbb{E}_1^1,\\&\hat{\Gamma}_i^1=He(M_1^T\tilde{P}_iN_1)+2\lambda M_1^T\tilde{P}_iM_1-\frac{e_\tau}{\bar{\tau}}\mathbb{I}_1^T\tilde{\mathcal{Q}}_{2i}\mathbb{I}_1+\tilde{\Lambda}_i^1,\\&\tilde{\Lambda}_i^1=diag\{\tilde{\Lambda}_{1i}^1,\tilde{\Lambda}_{2i}^1,0_5,\tilde{\Lambda}_{4i}^1,\tilde{\Lambda}_{5i}^1,\tilde{\Lambda}_{6i}^1,\tilde{\Lambda}_{7i}^1,\tilde{\Lambda}_{8i}^1,\tilde{\Lambda}_{9i}^1,\tilde{\Lambda}_{10i}^1\},\\&\tilde{\Lambda}_{1i}^1=\bar{\tau}\tilde{Q}_{2i},\quad\tilde{\Lambda}_{2i}^1=\tilde{Q}_{1i}+\tilde{U}_{1i}+\bar{\theta}\tilde{R}_{1i}+\tilde{U}_{2i}+\bar{\eta}\tilde{R}_{2i},\\&\tilde{\Lambda}_{4i}^1=-e_\tau\tilde{Q}_{1i},\quad\tilde{\Lambda}_{5i}^1=-e_\theta\tilde{U}_{1i},\quad\tilde{\Lambda}_{6i}^1=-e_\eta\tilde{U}_{2i},\\&\tilde{\Lambda}_{7i}^1=-\frac{e_\theta}{\bar{\theta}}\mathbb{K}^T\tilde{\mathscr{R}}_{1i}\mathbb{K},\ \tilde{\mathscr{R}}_{1i}=\tilde{\mathfrak{R}}_{1i}\otimes W_\kappa,\\&\tilde{\Lambda}_{8i}^1=-\frac{e_\eta}{\bar{\eta}}\mathbb{K}^T\tilde{\mathscr{R}}_{2i}\mathbb{K},\ \tilde{\mathscr{R}}_{2i}=\tilde{\mathfrak{R}}_{2i}\otimes W_\kappa,\\&\tilde{\Pi}_i^2=\tilde{\Gamma}_i^2+\mathbb{I}_4^T\tilde{\Phi}_i\mathbb{I}_4+He(\tilde{\mathscr{Y}}_i^2\tilde{\mathscr{G}}_i^2),\ \tilde{\Lambda}_{9i}^1=-\gamma_i^2I,\\&\tilde{\mathscr{Y}}_i^2=(\mu_1\mathbb{E}_1^2+\mu_2\mathbb{E}_2^2)^T,\ \tilde{\Lambda}_{10i}^1=\rho^2\mathcal{Z}_i-2\rho G_i,\\&\tilde{\mathscr{G}}_i^2=A_iX_i\mathbb{E}_2^2-B_iL_i\mathbb{E}_3^2+\frac{1}{h}B_iL_iC_i\mathbb{I}_3\\&\qquad+F_i\mathbb{E}_{11+4\kappa}^2+B_iL_iE_{12+4\kappa}^2-X_i\mathbb{E}_1^2,\\&\tilde{\Gamma}_i^2=He(M_2^T\tilde{P}_iN_2)+2\lambda M_2^T\tilde{P}_iM_2-\frac{e_\tau}{\bar{\tau}}\mathbb{I}_2^T\tilde{\mathcal{Q}}_{2i}\mathbb{I}_2+\tilde{\Lambda}_i^2,\\&\tilde{\Lambda}_i^2=diag\{\tilde{\Lambda}_{1i}^1,\tilde{\Lambda}_{2i}^1,0_2,\tilde{\Lambda}_{4i}^1,\tilde{\Lambda}_{5i}^1,\tilde{\Lambda}_{6i}^1,\tilde{\Lambda}_{7i}^1,\tilde{\Lambda}_{8i}^1,\tilde{\Lambda}_{9i}^1,\tilde{\Lambda}_{10i}^1\},\\&\tilde{\Phi}_i=\begin{bmatrix}-\tilde{\Psi}_i&0_{2,5}\\0_{5,2}&\frac{\sigma_i}{h^2}C_i^T\tilde{\Psi}_iC_i\end{bmatrix}.\end{aligned}$$

In addition, the controller gain is obtained as $K_i=L_iG_i^{-1}$.

Proof: Using Schur complement to (17), we have

$$\begin{bmatrix}\Pi_i^1&\mathbb{E}_2^{1\,T}C_i^T&\mathbb{E}_2^{1\,T}(\nu D_iC_i)^T\\ *&-I&0\\ *&*&-\nu I\end{bmatrix}<0.\tag{52}$$

Define $X_i=Y_i^{-1}$, $\tilde{R}_{1i}=X_iR_{1i}X_i$, $\tilde{R}_{2i}=X_iR_{2i}X_i$, $\tilde{U}_{1i}=X_iU_{1i}X_i$, $\tilde{U}_{2i}=X_iU_{2i}X_i$, $\tilde{Q}_{1i}=X_iQ_{1i}X_i$, $\tilde{Q}_{2i}=X_iQ_{2i}X_i$, $\tilde{S}_i=X_iS_iX_i$, $\tilde{S}_{1i}=X_iS_{1i}X_i$, $\tilde{S}_{2i}=X_iS_{2i}X_i$, $\tilde{\Psi}_i=G_i\Psi_iG_i$, $\tilde{P}_i=(I_{2\kappa+3}\otimes X_i)P_i(I_{2\kappa+3}\otimes X_i)$, $G_iC_i=C_iX_i$ and $L_iC_i=K_iC_iX_i$.

TABLE II
SYSTEM PARAMETERS

Parameters	Area 1	Area 2	Area 3
$\mathscr{D}_i$	1.8	1.5	1.2
$\mathscr{M}_i$	12	12	12
$\mathscr{T}_{gi}$	0.35	0.4	0.3
$\mathscr{T}_{ti}$	0.2	0.17	0.15
$\mathscr{R}_{fi}$	0.05	0.05	0.05
β_i	61.8	51.5	61.2
	$\mathscr{T}_{12}=0.2$	$\mathscr{T}_{23}=0.12$	$\mathscr{T}_{31}=0.25$

Pre- and post-multiplying (17) from both sides with matrix $\mathbb{X}_i = diag\{\boldsymbol{X}_i, \boldsymbol{X}_i, \boldsymbol{X}_i, \boldsymbol{X}_i, \boldsymbol{X}_i, \boldsymbol{X}_i, I_{\kappa+1}\otimes \boldsymbol{X}_i, I_{\kappa+1}\otimes \boldsymbol{X}_i, I, \boldsymbol{G}_i, I, I\}$ and its transpose $\mathbb{X}_i^T$, one has

$$\begin{bmatrix} \hat{\Pi}_i^1 & \mathbb{E}_2^{1\,T}\boldsymbol{X}_i\boldsymbol{C}_i^T & \mathbb{E}_2^{1\,T}\boldsymbol{X}_i(\nu\boldsymbol{D}_i\boldsymbol{C}_i)^T \\ * & -I & 0 \\ * & * & -\nu I \end{bmatrix} < 0, \tag{53}$$

where

$$\hat{\Pi}_i^1 = \hat{\Gamma}_i^1 + He(\mathscr{Y}_i^1\mathscr{C}_i^1), \quad \hat{\Lambda}_{10i}^1 = -\boldsymbol{G}_iZ_i\boldsymbol{G}_i$$
$$\hat{\Gamma}_i^1 = He(\boldsymbol{M}_1^T\tilde{P}_i\boldsymbol{N}_1) + 2\lambda\boldsymbol{M}_1^T\tilde{P}_i\boldsymbol{M}_1 - e_\tau\mathbb{I}_1^T\tilde{\mathcal{Q}}_{2i}\mathbb{I}_1 + \hat{\Lambda}_i^1,$$
$$\hat{\Lambda}_i^1 = diag\{\tilde{\Lambda}_{1i}^1, \tilde{\Lambda}_{2i}^1, 0_5, \tilde{\Lambda}_{4i}^1, \tilde{\Lambda}_{5i}^1, \tilde{\Lambda}_{6i}^1, \tilde{\Lambda}_{7i}^1, \hat{\Lambda}_{8i}^1\}.$$

Adopting the inequality $-\boldsymbol{G}_iZ_i\boldsymbol{G}_i \le \rho^2 Z_i^{-1} - 2\rho\boldsymbol{G}_i$ to (53), one has (49) by defining a new variable $\mathcal{Z}_i = Z_i^{-1}$.

By the similar way above, (48) and (50) can be derived.

Next, based on the control design approach [20], one gets

$$(\boldsymbol{G}_i\boldsymbol{C}_i - \boldsymbol{C}_i\boldsymbol{X}_i)^T(\boldsymbol{G}_i\boldsymbol{C}_i - \boldsymbol{C}_i\boldsymbol{X}_i) = 0. \tag{54}$$

With the help of Schur complement, (54) is transformed as the optimization issue (51). Thus, the proof is fulfilled. ■

IV. EXAMPLE

In this example, similar to [12], [15], we consider a three-area power system, the parameters of which are given in Table II.

These parameters can be imitated by choosing the values of resistors and capacitors given in Table III.

Similar to [20], a tangent function satisfying the condition (12) is selected as the mathematical expression that generates the deception attack. Then, the deception attack $\boldsymbol{d}_i(t) = [0.3tanh(\boldsymbol{y}_{i1}(t)); 0.3tanh(\boldsymbol{y}_{i2}(t))]$ is considered, and we have $\|\boldsymbol{d}_i(t)\|_2 \le \|\boldsymbol{D}_i\boldsymbol{C}_i\boldsymbol{x}_i(t)\|_2$ with $\boldsymbol{D}_i = 0.3I_2$. The other parameters are selected as $\sigma_i = 0.1$, $h = 0.025$, $\tau = 0.005$, $\mu_1 = 0.06$, $\mu_2 = 10$, $\delta = 0.01$, $\rho = 0.5$ and $\gamma_i = 10$ for $i = 1, 2, 3$. The time-varying communication delay is a random variable satisfies uniform distribution with upper bound $\bar{\theta} = 0.03$.

To illustrate the effectiveness of the developed event-triggered controller against deception attacks, two cases are considered as follows:

TABLE III
THE VALUES OF RESISTORS AND CAPACITORS

Parameters	Area 1	Area 2	Area 3
R_{l1i}	$1.8k\Omega$	$1.5k\Omega$	$1.2k\Omega$
R_{l2i}	$1k\Omega$	$1k\Omega$	$1k\Omega$
C_{li}	$12mF$	$12mF$	$10mF$
R_{gi}	$1k\Omega$	$1k\Omega$	$1k\Omega$
C_{gi}	$0.35mF$	$0.4mF$	$0.3mF$
R_{ti}	$1k\Omega$	$1k\Omega$	$1k\Omega$
C_{ti}	$0.2mF$	$0.17mF$	$0.15mF$
R_{f1i}	$0.05k\Omega$	$0.05k\Omega$	$0.05k\Omega$
R_{f2i}	$1k\Omega$	$1k\Omega$	$1k\Omega$
R_{a1i}	$6.18k\Omega$	$5.15k\Omega$	$6.12k\Omega$
R_{a2i}	$0.1k\Omega$	$0.1k\Omega$	$0.1k\Omega$
R_{bi}	$1k\Omega$	$1k\Omega$	$1k\Omega$
C_{ci}	$4mF$	$5mF$	$8.33mF$

Case A: the event-triggered controller is designed without considering the effect of deception attacks. Under this case, by removing the corresponding rows and columns related to $\boldsymbol{d}(t)$ in Theorem 2, the controller gain and triggering matrix are solved as:

$$\boldsymbol{K}_1 = [\,0.2159 \quad -0.1765\,], \ \Psi_1 = \begin{bmatrix} 0.3091 & -0.0310 \\ -0.0310 & 0.1772 \end{bmatrix};$$
$$\boldsymbol{K}_2 = [\,0.3308 \quad -0.0657\,], \ \Psi_2 = \begin{bmatrix} 0.3093 & -0.0471 \\ -0.0471 & 0.1832 \end{bmatrix};$$
$$\boldsymbol{K}_3 = [\,0.2627 \quad -0.0951\,], \ \Psi_3 = \begin{bmatrix} 0.3035 & -0.0343 \\ -0.0343 & 0.1663 \end{bmatrix};$$

Case B: the event-triggered controller gain is designed by considering the effect of deception attacks. In this case, they are derived by Theorem 2 as:

$$\boldsymbol{K}_1 = [\,-0.1779 \quad -0.0832\,], \ \Psi_1 = \begin{bmatrix} 1.7485 & -0.0529 \\ -0.0529 & 1.3877 \end{bmatrix};$$
$$\boldsymbol{K}_2 = [\,-0.1415 \quad -0.0252\,], \ \Psi_2 = \begin{bmatrix} 2.0737 & -0.1344 \\ -0.1344 & 1.4293 \end{bmatrix};$$
$$\boldsymbol{K}_3 = [\,-0.1540 \quad -0.0301\,], \ \Psi_3 = \begin{bmatrix} 1.6063 & -0.0896 \\ -0.0896 & 1.4081 \end{bmatrix}.$$

The simulation is executed in Matlab/Simulink environment. The part of power system and the part of controller are imitated by some analog circuits, which are simulated by using the special modules provided by Simcape toolbox of Simulink. In Fig. 3, some resistors, capacitors and operational amplifiers are utilized to imitate the power system. The time-varying delays induced by communication network are implemented via the general modules (variable time delay and uniform random number) provided by Simulink. The initial conditions are taken as $\boldsymbol{x}_1(0) = [\,0.3 \quad 0 \quad 0.2 \quad 0 \quad 0\,]^T$, $\boldsymbol{x}_2(0) = [\,-0.3 \quad 0 \quad 0.1 \quad 0 0\,]^T$, $\boldsymbol{x}_3(0) = [\,-0.2 \quad 0 \quad 0.2 \quad 0 \quad 0\,]^T$ and the simulation step is $0.0025\ s$. Due to the random changes of users, the load

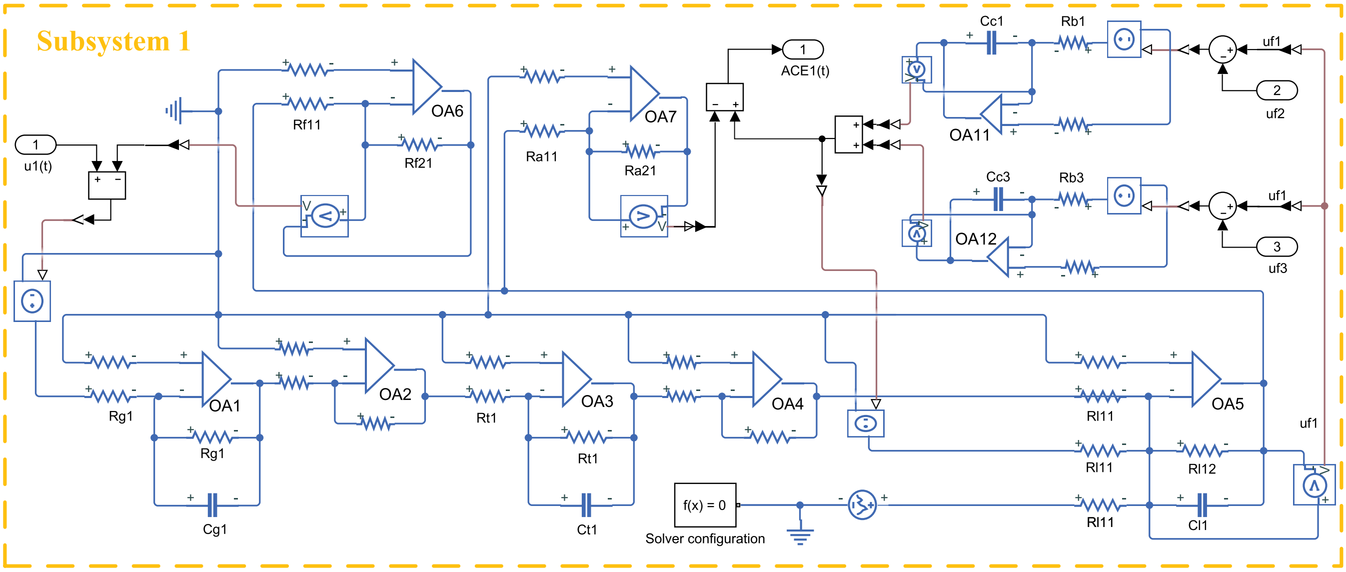

Fig. 3. The simulation framework of subsystem 1 of a multi-area power system imitated by circuit systems.

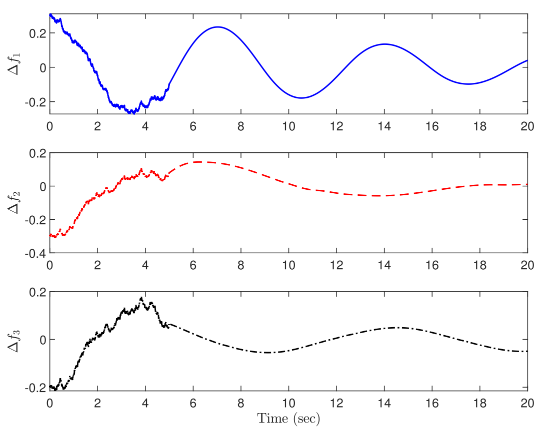

Fig. 4. Case A: Δf_i of three areas.

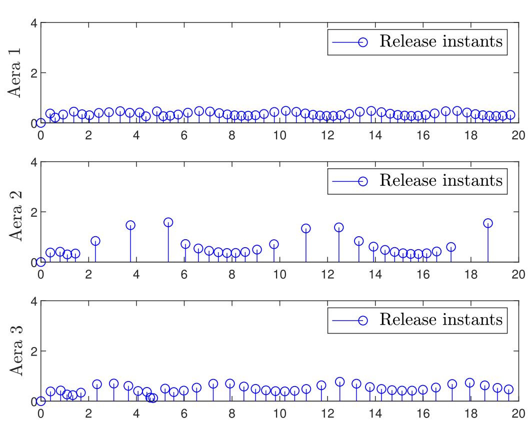

Fig. 5. Case A: Release instants of three areas.

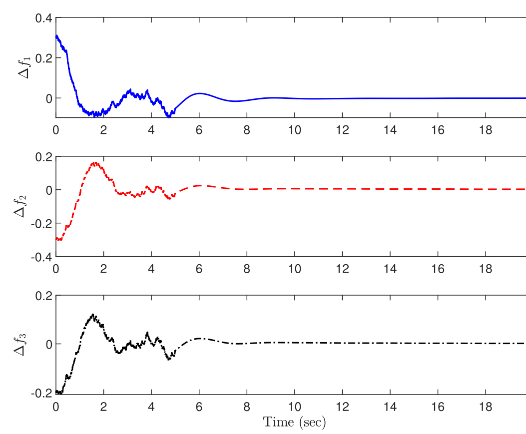

Fig. 6. Case B: Δf_i of three areas.

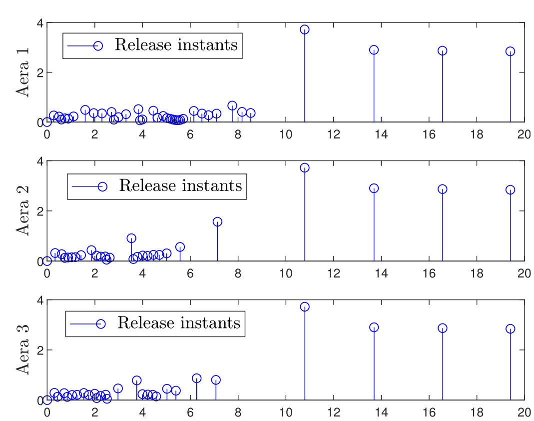

Fig. 7. Case B: Release instants of three areas.

TABLE IV
H_∞ PERFORMANCE INDICES γ_i, $i = 1, 2, 3$

	γ_1	γ_2	γ_3
Our method	5.8795	3.4996	5.4052
Method in [20]	6.6010	5.0227	6.0542

TABLE V
THE NUMBER OF TRIGGERED EVENTS: $\mathcal{N}$

	Aera 1	Aera 2	Aera 3
METM (7)	43	32	38
ETM (8) in [15]	79	55	59

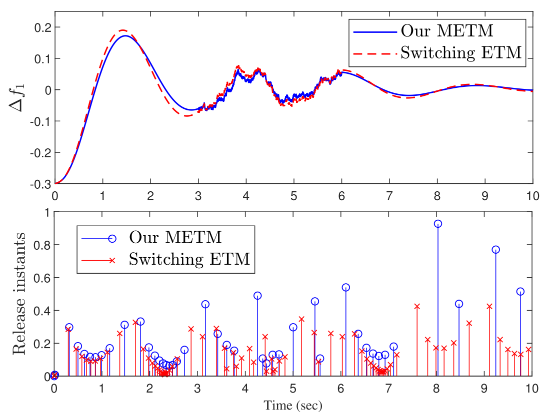

Fig. 8. Δf_1 and release instants under different ETMs.

disturbance is taken as $u_{di}(t) = a(t)$ for $0 < t < 5\ s$ ($u_{di}(t) = 0$ for $t \geq 5\ s$), where $a(t)$ is a random variable subject to the uniform distribution and $|a(t)| \leq 20$. The responses of the frequency and release instants under Case A and Case B are shown in Fig. 4 - Fig. 7, respectively.

From Fig. 4 and Fig. 6, one can see that better control performance and fewer triggering times are obtained by our event-triggered LFC method (Case B) than by the method without introducing the deception attacks into the controller design (Case A). To be specific, in Case A, the rise time of three areas is about $4\ s$ and the settling time is larger than $20\ s$. In Case B, however, the rise time is about $1.8\ s$ and the settling time is about $8\ s$. Note that both the rise time and the settling time in Case B are much smaller than the values in Case A.

To illustrate the advantage of our method without requiring the Lyapunov matrix P_i to be positive over the conventional method with $P_i > 0$ in [20], the values of the H_∞ performance indices for three control areas obtained by them are produced in Table IV. Based on the table, one observers that smaller H_∞ performance indices can be obtained by our method, which is less conservative than the method in [20].

In addition, to demonstrate the merit of the proposed METM (7), the comparison results with the existing switching ETM (8) are produced as follows.

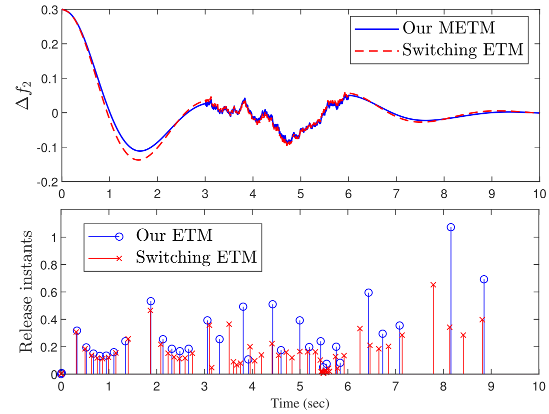

Fig. 9. Δf_2 and release instants under different ETMs.

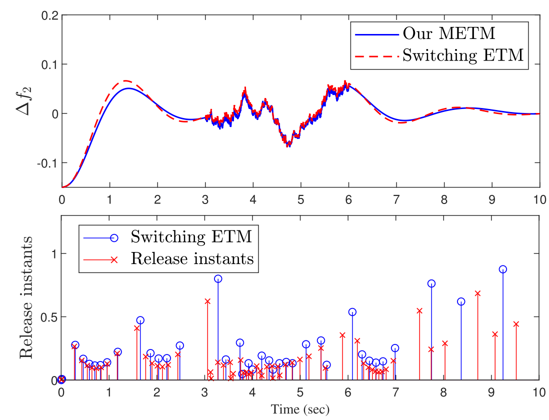

Fig. 10. Δf_3 and release instants under different ETMs.

Here, the same parameters, deception attacks in the above simulation are chosen. The external disturbance is considered as $u_{di}(t) = a(t)$ for $3 < t < 6\ s$ (otherwise, $u_{di}(t) = 0$). For three control areas, the responses of the frequency and the release instants under different ETMs are depicted in Fig. 8 - Fig. 10, respectively. The number of triggered events ($\mathcal{N}$) under different ETMs is derived in Table V.

According to these figures and Table V, one observes that almost the same responses of the area frequency deviation Δf_i are performed by these different ETMs. However, the amounts of triggered events for three control areas obtained via our proposed METM are decreased by 45.57%, 41.82% and 35.59% compared with the results produced via the existing switching ETM, respectively. This implies that with the introduction of the historic measured output, fewer control signals are triggered to guarantee the stability of the power systems and more network resources are saved than the existing ETM.

V. CONCLUSION

This paper has studied the decentralized memory-event-triggered H_∞ LFC of multi-area power systems subject to deception attacks and communication delays. Some circuits were adopted to simulate the dynamics of governor, turbine and power generator. To decrease the update times of control actions, the mean of past outputs was employed to construct the triggering rule. Then, a switched distributed delay system model was established to represent the power systems with deception attacks and communication delays under METM. By choosing a new LKF dependent on the distributed delay terms, sufficient stability and stabilization conditions were provided to be resilient against limited bandwidth and cyber-attacks. Furthermore, a circuit system was built up and simulated in the Matlab/Simulink to show the advantages of the presented strategy.

References

[1] X. Lou, D. K. Yau, R. Tan, and P. Cheng, "Cost and pricing of differential privacy in demand reporting for smart grids," *IEEE Trans. Netw. Sci. Eng.*, vol. 7, no. 3, pp. 2037–2051, Sep. 2020.

[2] X. Shangguan *et al.*, "Wu robust load frequency control for power system considering transmission delay and sampling period," *IEEE Trans. Ind. Inform.*, vol. 17, no. 8, pp. 5292–5303, Aug. 2021.

[3] K. Liao and Y. Xu, "A Robust load frequency control scheme for power systems based on second-order sliding mode and extended disturbance observer," *IEEE Trans. Ind. Inform.*, vol. 14, no. 7, pp. 3076–3086, Nov. 2017.

[4] D. Rerkpreedapong, A. Hasanovic, and A. Feliachi, "Robust load frequency control using genetic algorithms and linear matrix inequalities," *IEEE Trans. Power Syst.*, vol. 18, no. 2, pp. 855–861, May 2003.

[5] T. Pham, H. Trinh, and L. Hien, "Load frequency control of power systems with electric vehicles and diverse transmission links using distributed functional observers," *IEEE Trans. Smart Grid*, vol. 7, no. 1, pp. 238–252, Jan. 2016.

[6] L. Jiang, W. Yao, Q. Wu, J. Wen, and S. Cheng, "Delay-dependent stability for load frequency control with constant and time-varying delays," *IEEE Trans. Power Syst.*, vol. 27, no. 2, pp. 932–941, May 2012.

[7] S. Yan, M. Shen, S. K. Nguang, and G. Zhang, "Event-triggered H_∞ control of networked control systems with distributed transmission delay," *IEEE Trans. Autom. Control*, vol. 65, no. 10, pp. 4295–4301, Oct. 2020.

[8] Z. Gu, C. K. Ahn, D. Yue, and X. Xie, "Event-triggered H_∞ filtering for T-s fuzzy-model-based nonlinear networked systems with multi-sensors against DoS attacks," *IEEE Trans. Cybern*, to be published, doi: 10.1109/TCYB.2020.3030028.

[9] X. Jin, D. Wei, W. He, L. Kocarev, and Y. Tang, J. Kurths, "Twisting-based finite-time consensus for euler-lagrange systems with an event-triggered strategy," *IEEE Trans. Netw. Sci. Eng.*, vol. 7, no. 3, pp. 1007–1018, Sep. 2020.

[10] S. Yan, S. K. Nguang, Z. Gu, "H_∞ weighted integral event-triggered synchronization of neural networks with mixed delays," *IEEE Trans. Ind. Inform.*, vol. 17, no. 4, pp. 2365–2375, Apr. 2021.

[11] Z. Gu, P. Shi, D. Yue, S. Yan, and X. Xie, "Memory-based continuous event-triggered control for networked T-S fuzzy systems against cyber-attacks," *IEEE Trans. Fuzzy Syst.*, to be published, doi: 10.1109/TFUZZ.2020.3012771.

[12] S. Wen, X. Yu, Z. Zeng, and J. Wang, "Event-triggering load frequency control for multiarea power systems with communication delays," *IEEE Trans. Ind. Electron.*, vol. 63, no. 2, pp. 1308–1317, Feb. 2016.

[13] T. N. Pham, S. Nahavandi, H. Trinh, and K. P. Wong, "Static output feedback frequency stabilization of time-delay power systems with coordinated electric vehicles state of charge control," *IEEE Trans. Power Syst.*, vol. 32, no. 5, pp. 3862–3874, Sep. 2017.

[14] Z. Wu, H. Mo, J. Xiong, and M. Xie, "Adaptive event-triggered observer-based output feedback $\updownarrow_\infty$ load frequency control for networked power systems," *IEEE Trans. Ind. Inform.*, vol. 16, no. 6, pp. 3952–3962, Jun. 2020.

[15] S. Saxena and E. Fridman, "Event-triggered load frequency control via switching approach," *IEEE Trans. Power Syst.*, vol. 35, no. 6, pp. 4484–4494, Nov. 2020.

[16] A. Selivanov and E. Fridman, "Event-triggered H_∞ control: A switching approach," *IEEE Trans. Autom. Control*, vol. 61, no. 10, pp. 3221–3226, Oct. 2016.

[17] S. H. Mousavi and H. J. Marquez, "Integral-based event triggering controller design for stochastic LTI systems via convex optimisation," *Int. J. Control*, vol. 89, no. 7, pp. 1416–1427, Jan. 2016.

[18] X. Yan, Y. Liu, D. Huang and M. Jia, "A new approach to health condition identification of rolling bearing using hierarchical dispersion entropy and improved laplacian score," *Struct. Health Monit*, vol. 20, no. 3, pp. 1169–1195, 2021.

[19] X. Wang, Z. Fei, H. Gao, and J. Yu, "Integral-based event-triggered fault detection filter design for unmanned surface vehicles," *IEEE Trans. Ind. Informat.*, vol. 15, no. 10, pp. 5626–5636, Oct. 2019.

[20] E. Tian and C. Peng, "Memory-based event-triggering H_∞ load frequency control for power systems under deception attacks," *IEEE Trans. Cybern.*, vol. 50, no. 11, pp. 4610–4618, Nov. 2020.

[21] Y. Tang, D. Zhang, P. Shi, W. Zhang, and F. Qian, "Event-based formation control of multi-agent systems under denial-of-service attacks," *IEEE Trans. Autom. Control*, vol. 66, no. 1, pp. 452–459, Jan. 2021.

[22] P. Dai, W. Yu, H. Wang, G. Wen, and Y. Lv, "Distributed reinforcement learning for cyber-physical system with multiple remote state estimation under DoS attacker," *IEEE Trans. Netw. Sci. Eng.*, vol. 7, no. 4, pp. 3212–3222, Oct.–Dec. 2020.

[23] T. Zhang and D. Ye, "False data injection attacks with complete stealthiness in cyber-physical systems: A self-generated approach," *Automatica*, vol. 120, pp. 109–117, Oct. 2020.

[24] Z. Gu, J. H. Park, D. Yue, Z. Wu, and X. Xie, "Event-triggered security output feedback control for networked interconnected systems subject to cyber-attacks," *IEEE Trans. Syst. Man, Cybern. Syst.*, to be published, doi: 10.1109/TSMC.2019.2960115.

[25] C. Peng, J. Li, and M. Fei, "Resilient event-triggering h_∞ load frequency control for multi-area power systems with energy-limited DoS attacks," *IEEE Trans. Power Syst.*, vol. 32, no. 5, pp. 4110–4118, Sep. 2017.

[26] X. Zhou, Z. Gu, and F. Yang, "Resilient event-triggered output feedback control for load frequency control systems subject to cyber attacks," *IEEE Access*, vol. 7, pp. 58951–58958, May 2019.

[27] J. Liu, Y. Gu, L. Zha, Y. Liu, and J. Cao, "Event-triggered h_∞ load frequency control for multiarea power systems under hybrid cyber attacks,"*IEEE Trans. Syst., Man, Cybern. Syst.*, vol. 49, no. 8, pp. 1665–1678, Aug. 2019.

[28] Z. Fei, C. Guan, and H. Gao, "Exponential synchronization of networked chaotic delayed neural network by a hybrid event trigger scheme," *IEEE Trans. Neural Netw. Learn. Syst.*, vol. 29, no. 6, pp. 2558–2567, Jun. 2018.

[29] Z. Fei, C. Guan, and X. Zhao, "Event-triggered dynamic output feedback control for switched systems with frequent asynchronism," *IEEE Trans. Autom. Control*, vol. 65, no. 7, pp. 3120–3127, Jul. 2020.

[30] X. Wang, Z. Fei, H. Yan, and Y. Xu, "Dynamic event-triggered fault detection via zonotopic residual evaluation and its application to vehicle lateral dynamics," *IEEE Trans. Ind. Inform.*, vol. 16, no. 11, pp. 6952–6961, Nov. 2020.

[31] Q. Feng, S. K. Nguang, and W. Perruquetti, "Dissipative stabilization of linear systems with time-varying general distributed delays," *Automatica*, vol. 122, Dec. 2020, Art. no. 109227.

[32] N. J. Higham, "*The Matrix Computation Toolbox for MATLAB (Version 1.0)*, *Manchester Centre Comput. Mathematics*, 2002.

[33] P. Park, J. W. Ko, and C. Jeong, "Reciprocally convex approach to stability of systems with time-varying delays," *Automatica*, vol. 47, no. 1, pp. 235–238, Jan. 2011.

[34] Y. Wang, L. Xie, and C. E. DeSouza, "Robust control of a class of uncertain nonlinear systems," *Syst. Control Lett.*, vol. 19, no. 2, pp. 139–149, Aug. 1992.

[35] A. Seuret, F. Gouaisbaut, and Y. Ariba, "Complete quadratic lyapunov functionals for distributed delay systems," *Automatica*, vol. 62, pp. 168–176, Dec. 2015.

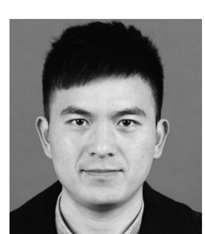

Shen Yan received the B.E. and Ph.D. degrees from the College of Electrical Engineering and Control Science, Nanjing Tech University, Nanjing, China. He is currently a Lecturer with the College of Mechanical and Electronic Engineering, Nanjing Forestry University, Nanjing, China. His current research interests include networked control systems, power systems, and event-triggered control.

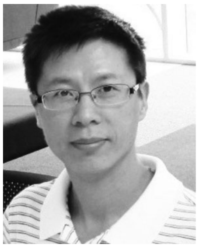

Zhou Gu received the B.S. degree from North China Electric Power University, Beijing, China, in 1997, and the M.S. and Ph.D. degrees in control science and engineering from the Nanjing University of Aeronautics and Astronautics, Nanjing, China, in 2007 and 2010, respectively. From 1996 to 2013, he was an Associate Professor with the School of Power engineering, Nanjing Normal University, Nanjing, China. He was a Visiting Scholar with Central Queensland University, Rockhampton, QLD, Australia and with The University of Manchester, Manchester, U.K. He is currently a Professor with Nanjing Forestry University, Nanjing, China. His current research interests include networked control systems, time-delay systems, reliable control, and their applications.

Ju H. Park (Senior Member, IEEE) received the Ph.D. degree in electronics and electrical engineering from the Pohang University of Science and Technology (POSTECH), Pohang, South Korea, in 1997. From May 1997 to February 2000, he was a Research Associate with Engineering Research Center-Automation Research Center, POSTECH. In March 2000, he joined Yeungnam University, Gyeongsan, South Korea, where he is currently the Chuma Chair Professor. He is the coauthor of the monographs *Recent Advances in Control and Filtering of Dynamic Systems with Constrained Signals (Springer-Nature 2018)* and the *Dynamic Systems With Time Delays: Stability and Control (Springer-Nature 2019)* and is the Editor of an edited volume *the Recent Advances in Control Problems of Dynamical Systems and Networks (Springer-Nature 2020)*. His research interests include robust control and filtering, neural or complex networks, fuzzy systems, multiagent systems, and chaotic systems. He has authored or coauthored a number of articles in these areas. He is a Fellow of the Korean Academy of Science and Technology, Seongnam-si, South Korea. He is also the Editor of the *International Journal of Control, Automation and Systems*. He is also a Subject Editor or Advisory Editor or an Associate Editor or an Editorial Board Member of several international journals, including the *IET Control Theory & Applications, Applied Mathematics and Computation, the Journal of The Franklin Institute, Nonlinear Dynamics, Engineering Reports, Cogent Engineering*, IEEE Transaction on Fuzzy Systems, IEEE Transaction on Neural Networks and Learning Systems, and IEEE Transaction on Cybernetics. Since 2015, he has been the recipient of the Highly Cited Researchers Award by Clarivate Analytics (formerly, Thomson Reuters) and listed in three fields, Engineering, Computer Sciences, and Mathematics, in 2019 and 2020.